https://doi.org/10.5194/egusphere-2026-4187
Preprint. Discussion started: 7 August 2026

From CMIP6 to eddy-rich models: does very-high resolution improve the representation of Mediterranean heavy precipitation events?

Ramiro I. Saurral[a,b,c,d], Anna Martín-Perellón[a], Diego A. Campos[a,e], Juan Jesús González-Alemán[f], Saskia Loosveldt-Tomas[a], and Pablo Ortega[a]

[a] Barcelona Supercomputing Center (BSC), Barcelona, Spain
[b] CONICET-Universidad de Buenos Aires. Centro de Investigaciones del Mar y la Atmósfera (CIMA), Buenos Aires, Argentina
[c] Universidad de Buenos Aires, Facultad de Ciencias Exactas y Naturales, Departamento de Ciencias de la Atmósfera y los Océanos, Buenos Aires, Argentina
[d] CNRS-IRD-CONICET-UBA. Instituto Franco-Argentino para el Estudio del Clima y sus Impactos (IRL 3351 IFAECI), Buenos Aires, Argentina
[e] Facultat de Física, Universitat de Barcelona, Barcelona, Spain
[f] Spanish State Meteorological Agency (AEMET), Department of Science, Madrid, Spain

Corresponding author: Ramiro I. Saurral (ramiro.saurral@bsc.es)

https://doi.org/10.5194/egusphere-2026-4187
Preprint. Discussion started: 7 August 2026

ABSTRACT

The Mediterranean region is a recognized climate-change hotspot where heavy precipitation events are frequently associated with cut-off lows (COLs). However, traditional climate models show limited skill in representing both the climatology of these systems and their relationship with extreme rainfall. Here, we assess the impact of horizontal resolution on the simulation of Mediterranean COLs and associated precipitation using four very-high-resolution simulations from the EERIE project and eighteen standard-resolution CMIP6 models, with ERA5 reanalysis as reference. Results show that all models underestimate COL frequency over the Mediterranean, although this bias is substantially reduced in the eddy-rich EERIE simulations, particularly over the western Mediterranean. Reanalysis indicates that COLs contribute to 20–40% of total precipitation across much of the region, but their importance increases markedly for upper-tail events, accounting for more than 60% of precipitation exceeding the 99th percentile over large areas. In contrast, CMIP6 models largely fail to reproduce this enhanced COL contribution to extremes. Several EERIE simulations, however, capture these observed relationships more realistically and produce substantially larger precipitation maxima associated with COLs. Future projections suggest a decrease in COL occurrence over the western and central Mediterranean, but contrasting responses in associated extreme precipitation emerge between EERIE and CMIP6 simulations. These results highlight the importance of very-high-resolution climate simulations for representing Mediterranean precipitation extremes and reveal persistent uncertainties in their future evolution.

Keywords: global climate modeling; very-high resolution; cut-off lows; extreme precipitation

https://doi.org/10.5194/egusphere-2026-4187
Preprint. Discussion started: 7 August 2026

1. Introduction

The Mediterranean region is widely recognized as one of the major climate-change hotspots worldwide due to the magnitude of the observed and projected temperature and precipitation trends (Cos et al., 2022; Giorgi, 2006; Lionello and Strascia, 2018; Tuel and Eltahir, 2020). A notable feature of these changes is the counterintuitive coexistence of a decline in mean precipitation and an increase in heavy precipitation events (HPEs) across large sectors of southern Europe and the Mediterranean basin (Chericoni et al., 2025; Senatore et al., 2026; Zappa et al., 2015). This apparent paradox is associated with both dynamic (Chericoni et al., 2025; Reale et al., 2022; Insua-Costa et al., 2022; Mastrantonas et al., 2021; Porcù et al., 2007; Saurral et al., 2025) and thermodynamic (Campos et al., 2026; Yuan et al., 2023) changes in the climate system at the regional scale.

From the dynamical side, mid- and upper-tropospheric cyclones forming in recent years over the Mediterranean have been responsible for impactful HPE over southern Europe (e.g., Calvo-Sancho et al., 2026; Campos et al., 2026; Ramonell et al., 2026; Saurral et al., 2026; Thompson et al., 2024). These systems, typically referred to as cut-off lows (COLs), are defined as synoptic-scale low-pressure systems that become detached from the progressive mid-latitude westerly flow. This segregation makes them move slowly and erratically for a few to several days (Palmen and Newton, 1969; Price and Vaughan, 1992), which frequently leads to prolonged multi-day threats of heavy rainfall. One such example is the COL that affected Valencia, in eastern Spain, during October 2024, with record-setting precipitation that was favoured by warm conditions in the Mediterranean Sea and the North Atlantic (Campos et al., 2026; Saurral et al., 2026). During this event, which occurred in a region of complex topography, precipitation maxima varied from around 700 mm in the mountain areas to less than 15 mm at the Valencia airport, separated by only 25 kilometers. Such sharp precipitation gradients are poorly represented in standard-resolution atmospheric models, but the challenge persists even at much finer spatial scales. Simulations of this event at 9 km resolution globally produced maxima of ~220 mm (Saurral et al., 2026), a significant underestimate that has been largely overcome with simulations performed with a regional model at 1 km resolution where precipitation exceeded 500 mm (Calvo-Sancho et al., 2026). In fact, convection-permitting resolutions tend to intensify precipitation extremes (Iles et al., 2020; Prein et al., 2015; Reder et al., 2022), although they may also increase uncertainty in upper-tail estimates (Caillaud et al., 2024; Müller et al., 2024).

Despite the substantial contribution of COLs to HPE over the Mediterranean and elsewhere (e.g., Choquehuanca et al., 2025; Jury, 2025; Nieto et al., 2005; Valenzuela et al., 2022), current global climate models have limited skill to represent their geographical and temporal distributions (Pinheiro et al., 2022), which limits their utility for future climate assessments and informed decision-making. In this regard, Saurral et al. (2025) analyzed the COL-HPE linkages over the Mediterranean region in standard-resolution climate models. The study highlighted on one hand the poor skill of most models to represent the centers of action of COLs over the region, and on the other hand a large underestimation in the amount of heavy precipitation associated with COLs. Furthermore, Cos et al. (2022) provided evidence that CMIP6 models perform comparably to, or worse than, their CMIP5 counterparts in the simulation of precipitation over southern Europe.

Recently, the rapid growth in computational resources paired with parallel advances in high resolution modeling has underpinned the capacity of modelling centers to conduct climate scale simulations with global coupled configurations capable of explicitly resolving mesoscale ocean eddies and their

https://doi.org/10.5194/egusphere-2026-4187
Preprint. Discussion started: 7 August 2026

interactions with the atmosphere (e.g., Chen et al., 2025; John et al., 2026). This leap forward in climate modelling, crystallized in recent initiatives such as the second phase of HighResMIP (Roberts et al., 2025) and Destination Earth (Doblas-Reyes et al., 2026), is expected to narrow down the uncertainty associated with the misrepresentation of fine-scale processes. However, studies investigating outputs from these numerical protocols have reached mixed conclusions. While a number of studies found significant improvements in numerical experiments performed at high resolution in features like the representation of atmospheric rivers and their variability (Nellikkattil et al., 2023), winter precipitation trends over Europe (Moreno-Chamarro et al., 2021) or tropical cyclone density (Vecchi et al., 2019), other studies found negligible impacts stemming from the increase in horizontal resolution on the patterns of tropical Pacific warming (Dhame et al., 2025) or the atmospheric response to sea ice loss (Streffing et al., 2021), among others. Therefore, the benefit of high and eddy-rich resolution in climate modelling seems to be, according to the evidence, dependent upon the variable under consideration, or the model considered. More systematic comparisons are therefore needed.

In the case of the ongoing European Eddy-Rich ESMs (EERIE) Horizon Europe project, the novelty is the adoption of global oceanic resolutions close to 10 km which allow to explicitly resolve the ocean eddies and associated interactions, potentially resulting in improvements in weather and climate simulations compared to CMIP6 standards. These simulations have only recently been completed, and studies on the quantification of their potential improvements are so far limited. In this study, we use outputs from EERIE simulations at both historical and future periods in order to assess their representation of Mediterranean COLs and the associated precipitation using CMIP6 models as a benchmark. The objective is twofold: to assess if eddy-rich simulations become more skillful to represent the frequency and distribution of COLs over the Mediterranean region, but also to determine if eddy-rich resolution is useful to capture the observed COL-extreme precipitation linkages over the region.

2. Data and methods

a. Reanalysis

ERA5 (Hersbach et al., 2020) reanalysis data is used for a complete physically-coherent characterization of precipitation-COL linkages over the Mediterranean region. This is based on the joint analysis of daily precipitation and 500 hPa-geopotential height (h500) fields. The identification of COLs is carried out following the methodology described later in this section. All the analysis is done at a resolution of 0.25º. For comparability against historical EERIE and CMIP6 model outputs, the period of analysis runs from January 1960 to December 2014. The region under study is the Mediterranean Sea, covering from 30ºN to 50ºN in latitude and from 10ºW to 40ºE in longitude. The location of the study region is depicted in Fig. 1c.

In parallel, and as an independent way to quantify the sensitivity of the results to the horizontal resolution of the reanalysis dataset, we perform a separate analysis using the NCEP-NCAR 1 (Kalnay et al., 1996) dataset at its native coarse horizontal resolution of 2.5º.

https://doi.org/10.5194/egusphere-2026-4187
Preprint. Discussion started: 7 August 2026

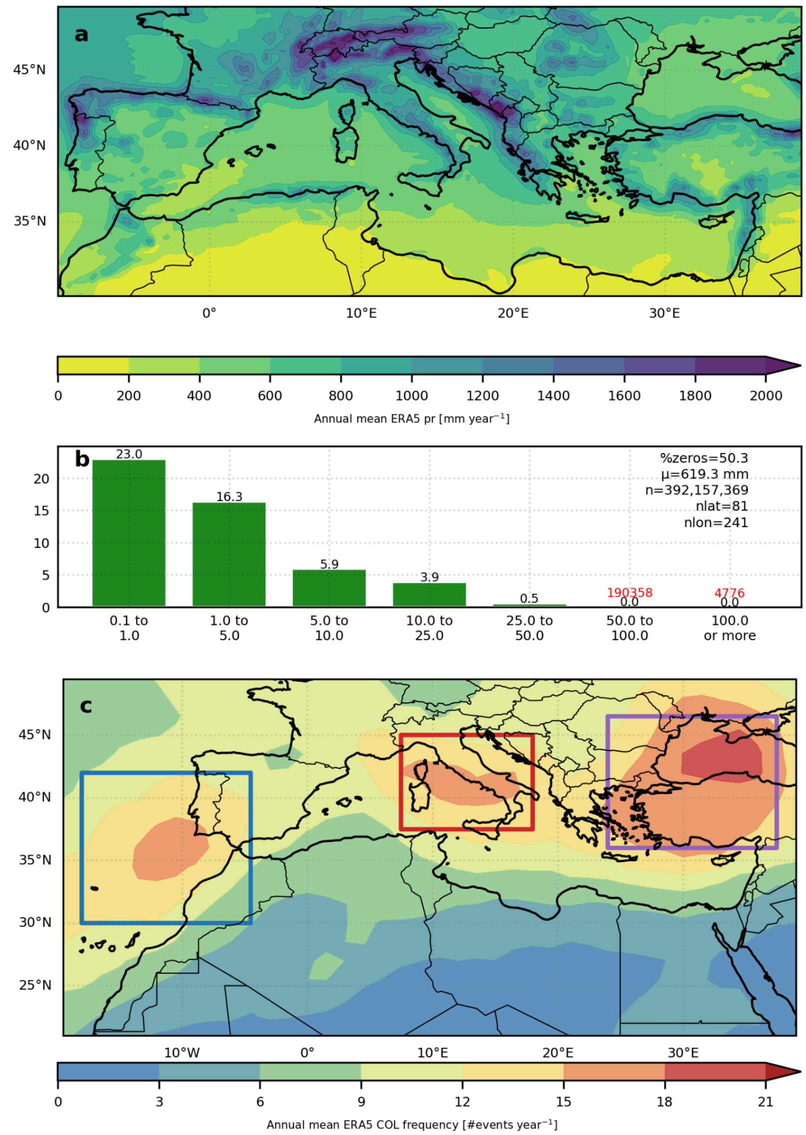

Figure 1 Climatology (period 1960-2014) of precipitation and COL frequency in ERA5 reanalysis over the Mediterranean region. (a) Annual mean precipitation (in mm year^{-1}) and (b) histograms of daily precipitation considering all the grid points included in (a) for bins [0.1 to 1.0), [1.0 to 5.0), [5.0 to 10.0), [10.0 to 25.0), [25.0 to 50.0), [50.0 to 100.0), and more than 100 mm day^{-1}. The numbers in black above each bar indicate the percentage of values in that bin, while numbers in red above the two highest bins indicate the number of grid points included in these categories. Also shown in the upper right corner is the percentage of zero-precipitation values (i.e., precipitation amounts of less than 0.1 mm day^{-1}; %zeros), the spatial average of precipitation (μ), the total number of precipitation data (number of days x number of latitudes x number of longitudes; n), and the number of latitudes and longitudes (nlat and nlon, respectively). (c) Annual mean frequency of COLs, in number of events per year. The coloured boxes indicate the three areas with highest COL frequency: WMed (blue), CMed (red) and EMed (purple).

https://doi.org/10.5194/egusphere-2026-4187
Preprint. Discussion started: 7 August 2026

b. Models

We consider two independent groups of experiments: one encompassing four eddy-rich (ER) EERIE models and another one including standard-resolution simulations from the eighteen CMIP6 models (Eyring et al., 2016) for which daily precipitation and h500 data were available. One ensemble member (r1i1p1f1) was considered per model for both EERIE and CMIP6. The models included in each group, along with the institutions that developed them and details on the atmospheric and oceanic resolutions, are listed in Table 1 for EERIE and in Table 2 for CMIP6. Also, one of the models contributing to EERIE (HadGEM3-GC5E) also had available a standard-resolution eddy-parameterized (EP) simulation, for which reason we included it in order to assess the impact of resolution on the same model. As in the case of the reanalyses, the data under consideration are daily fields of h500 and precipitation over the Mediterranean region.

We perform the analysis over a historical ("hist") period matching that of the reanalysis and also over future climate scenarios for both EERIE and CMIP6. Even though most of the CMIP6 models have climate projections extending all the way to the end of the present century, in this study the future is represented by the shorter period 2025-2050, limited by the end year of the EERIE simulations, which follow the HighResMIP protocol. In these future scenarios, a difference between the EERIE and CMIP6 datasets is the adoption of a single or various Shared Socioeconomic Pathways (SSPs): in the case of CMIP6 four SSPs (from smoother to more aggressive in terms of human fingerprints on climate) were available: SSP1-2.6, SSP2-4.5, SSP3-7.0 and SSP5-8.5, while the EERIE runs were only produced under SSP2-4.5.

Table 1 Characteristics of the EERIE models

ESM	Institution	Atmos resol	Ocean resol	References
ICON	MPI (Germany)	~10km	~5km	Hohenegger et al. (2023)
IFS-FESOM	AWI (Germany)	~9km	~5km	Rackow et al. (2025)
IFS-NEMO	BSC (Spain)	~9km	~9km	Rackow et al. (2025)
HadGEM3-GC5E-HH	Met Office (UK)	~20km	~9km	Xavier et al. (2023)
HadGEM3-GC5E-LL	Met Office (UK)	~250km	~100km	Xavier et al. (2023)

Table 2 Characteristics of the CMIP6 models

ESM	Institution (country)	Atmos resol	Ocean resol	References
ACCESS-CM2	CSIRO (Australia)	~135km	~25 to 100km	Bi et al. (2020)
BCC-CSM2-MR	BCC (China)	~100km	~30 to 100km	Wu et al. (2021)
CanESM5	CCCMA	~300km	~30 to 100km	Swart et al. (2019)

https://doi.org/10.5194/egusphere-2026-4187
Preprint. Discussion started: 7 August 2026

	(Canada)			
CESM2-WACCM	NCAR (US)	~100km	~30 to 100km	Danabasoglu et al. (2020)
CNRM-CM6-1-HR	CNRM (France)	~100km	~25km	Voldoire et al. (2019)
CNRM-CM6-1	CNRM (France)	~150km	~30 to 100km	Voldoire et al. (2019)
CNRM-ESM2-1	CNRM (France)	~150km	~30 to 100km	Séférian et al. (2019)
EC-Earth3	EC-Earth Consortium (EU)	~80km	~30 to 100km	Döscher et al. (2022)
FGOALS-g3	CAS (China)	~200km	~30 to 100km	Li et al. (2020)
IITM-ESM	IITM (India)	~200km	~30 to 100km	Swapna et al. (2018)
INM-CM5-0	INM (Russia)	~200km	~25km	Volodin et al. (2017)
IPSL-CM6A-LR	IPSL (France)	~250km	~30 to 100km	Boucher et al. (2020)
MPI-ESM-1-2-HR	MPI (Germany)	~100km	~40km	Müller et al. (2018)
MRI-ESM2-0	MRI (Japan)	~120km	~30 to 100km	Yukimoto et al. (2019)
NorESM2-LM	NCC (Norway)	~240km	~100km	Seland et al. (2020)
NorESM2-MM	NCC (Norway)	~120km	~100km	Seland et al. (2020)
TaiESM1	RCEC (Taiwan)	~100km	~100km	Lee et al. (2020)
UKESM1-0-LL	Met Office (UK)	~120km	~100km	Sellar et al. (2019)

c. COL detection algorithm

We identify COLs at daily time step using the detection method developed by Kasuga et al. (2021). This scheme has been extensively used for COL-related studies worldwide (e.g., Kasuga and Honda, 2025; Lupo et al., 2023; Saurral et al., 2025; Yamamoto et al., 2024) and works on a given pressure level. In our case, we used the 500-hPa isobaric level due to the largest portion of CMIP6 data availability. This choice should not have a significant impact on the results (Kasuga et al., 2021).

The scheme uses a 2D slope function and looks for local minima in h500 co-occurring with local maxima in the slope of the same variable (i.e., a minimum surrounded by sharp increases in h500 away from that minimum). According to sensitivity tests performed by Kasuga et al. (2021), the

https://doi.org/10.5194/egusphere-2026-4187
Preprint. Discussion started: 7 August 2026

detection scheme requires computing the slope in the zonal and meridional direction up to a distance R from the local minimum, with R varying from 200 to 2100 km. Other restrictions proposed by Kasuga et al. (2021) are also applied here in order to discard systems that are too small or too close to the equator. The method is applied to all grid points in the study area and for all the days within the study period (both for historical and future periods, considering the different SSPs when available), resulting in daily fields of COL locations. For a more detailed description of the detection algorithm, including examples, the reader is referred to Kasuga et al. (2021) and Lupo et al. (2023).

To provide fair comparisons between COL fields derived from ERA5, CMIP6 and EERIE models (all with different horizontal resolutions), all daily h500 fields were regridded into a regular 1.5-degree resolution before applying the detection scheme, which is suitable for COL detection while also removing sub-synoptic (smaller-scale) features (Kasuga et al., 2021).

d. Assessment of COL-precipitation linkages

Here we adapt the methodology developed by Pfahl and Wernli (2012) and refined by Catto et al. (2012) and Catto and Pfahl (2013) for the attribution of precipitation events to surface cyclones and fronts. In their case, they consider that a given precipitation event is triggered by any of these weather features if a surface cyclone or front is located within a distance of 5 degrees from the precipitation location. In our case, we build on previous studies on the association between COLs and precipitation over Chile (Muñoz and Shultz, 2021), South Africa (Favre et al., 2012) and the western Mediterranean (Saurral et al., 2026) and consider that a precipitation event is associated with a COL if a COL lies within 10 degrees to the west and within 5 degrees north/south of the grid point of the precipitation location. We performed sensitivity tests to this selection by placing the precipitation grid point at different locations within the box and found that the largest precipitation amounts triggered by COLs were achieved when using the selected box, providing confidence in the attribution procedure.

Under this selection, we define a contribution index (CI) of COLs to precipitation, considered as the number of days in which precipitation occurs in association with a COL divided by the total number of days with precipitation, regardless of the presence of a COL. We apply this definition to all precipitation days per grid point and also only to days exceeding specific precipitation percentiles, as a way to additionally assess the contribution of COLs to extreme rainy days. The selected percentiles are the 90th, 95th and 99th (P90, P95 and P99, respectively) computed over the entire historical period for ERA5 as well as for the EERIE and CMIP6 models. The computation of the percentiles is done individually at each grid point.

3. Results

a. COL-precipitation association in reanalysis

Annual precipitation over the Mediterranean region (Fig. 1a) shows a marked south-north gradient, varying from values below 200 mm year^{-1} over the north African coasts to maxima locally exceeding 2000 mm year^{-1} over parts of northern Italy and the Balkans. The distribution of daily precipitation within the study area (Fig. 1b) is dominated by days with either zero or low precipitation (95.6% of the data lying below 10 mm day^{-1}). On the other tail of the distribution, the fraction of days above 25 mm is as low as 0.5%, and a total of 4,776 records lay above 100 mm day^{-1}.

The annual-mean spatial distribution of COLs in ERA5 (Fig. 1c) is characterized by three well-defined maxima: one extending from the North Atlantic coasts of the Iberian Peninsula onto the

https://doi.org/10.5194/egusphere-2026-4187
Preprint. Discussion started: 7 August 2026

far western Mediterranean (WMed), another one centered over central Italy which also covers the Corsica and Sicily islands (central Mediterranean; CMed) and a third one that covers the far eastern Mediterranean as well as most of Turkey and the Black Sea (EMed). The frequency of COLs over these three areas is similar, albeit larger over EMed.

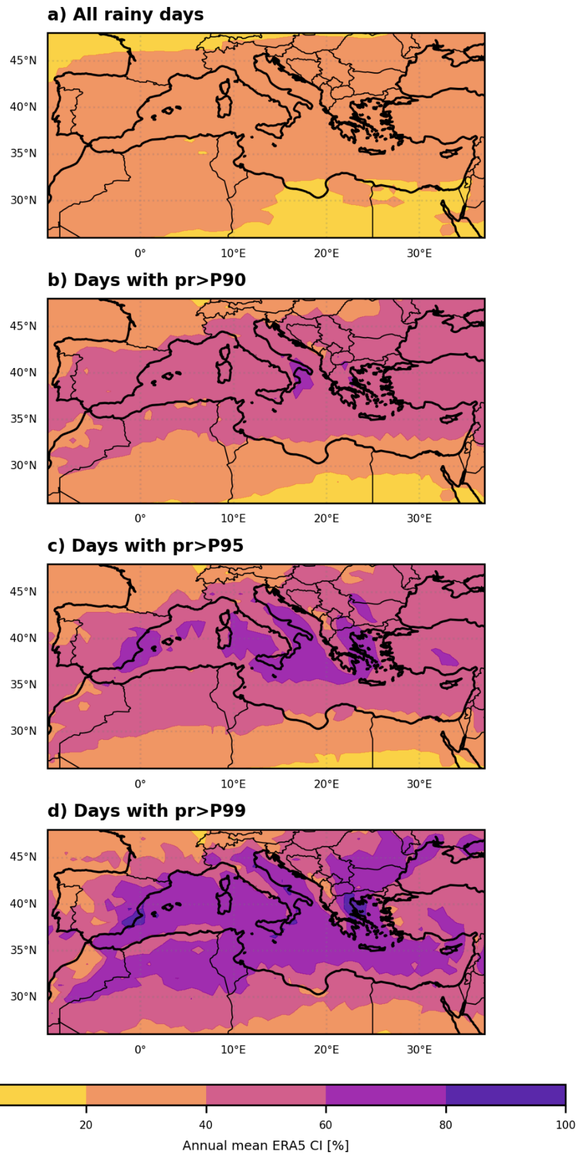

Figure 2 Spatial distribution of CI in ERA5 reanalysis (period 1960-2014) considering (a) all days with non-zero precipitation, and days exceeding (b) P90, (c) P95, and (d) P99. Units are %. See text for further details.

https://doi.org/10.5194/egusphere-2026-4187
Preprint. Discussion started: 7 August 2026

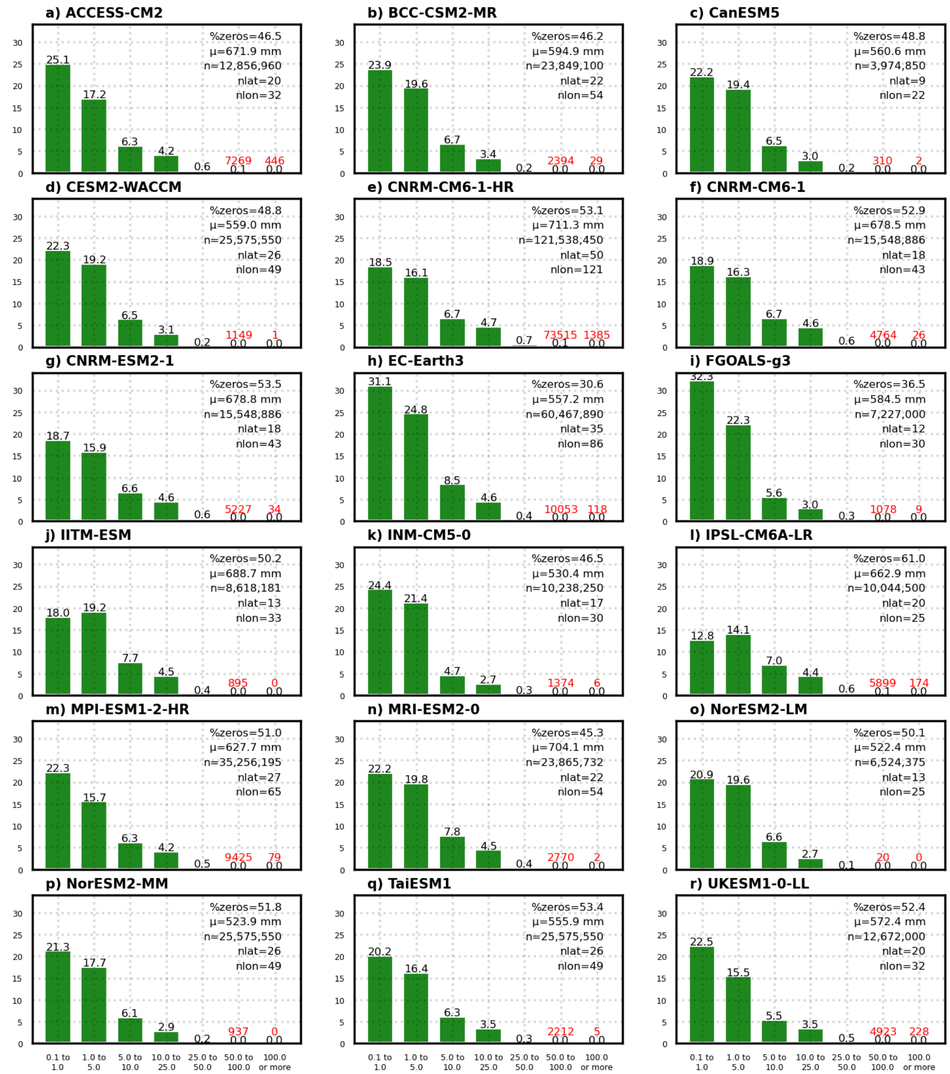

Figure 3 Histograms of historical (1960-2014) daily precipitation over the Mediterranean region in CMIP6 models for the same bins considered in Figure 1b. The numbers in black above each bar indicate the percentage of values in that bin, while numbers in red above the two highest bins indicate the number of grid points included in these categories. Also shown in the upper right corner is the percentage of zero-precipitation values (i.e., precipitation amounts of less than 0.1 mm day^{-1}; %zeros), the spatial average of precipitation (μ), the total number of precipitation data (number of days x number of latitudes x number of longitudes; n), and the number of latitudes and longitudes (nlat and nlon, respectively) for each model.

https://doi.org/10.5194/egusphere-2026-4187
Preprint. Discussion started: 7 August 2026

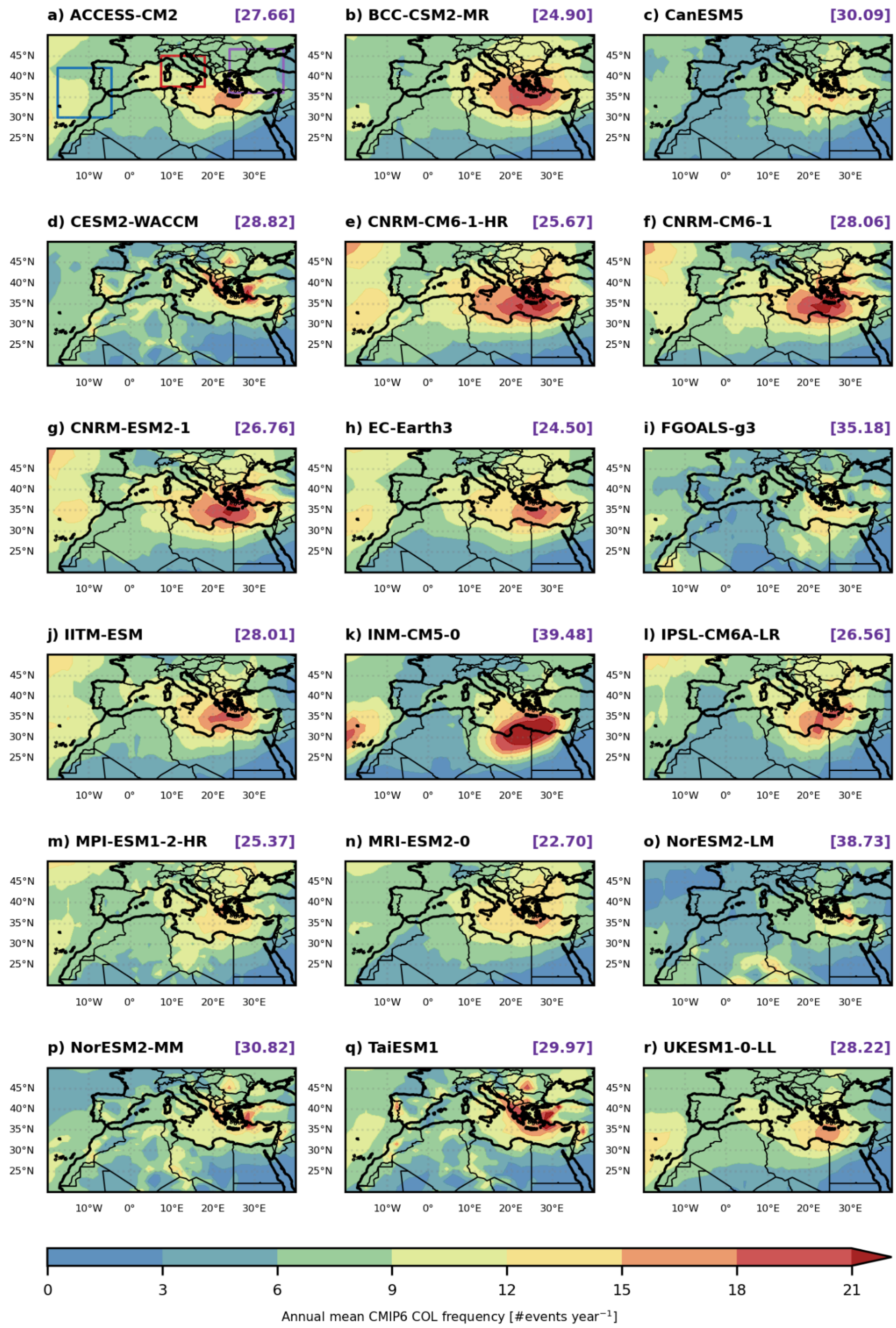

Figure 4 Annual-mean frequency of COLs in CMIP6 models in the historical period (1960-2014) over the Mediterranean region. Values are expressed in number of events per year. For reference, the location of boxes WMed, CMed and EMed is displayed in panel a. The number in purple in each plot indicates the area-weighted root mean square error computed against ERA5.

https://doi.org/10.5194/egusphere-2026-4187
Preprint. Discussion started: 7 August 2026

The CI fields computed from ERA5 data (Fig. 2) shows that between 20 and 40% of the annual precipitation over the Mediterranean Sea is triggered by COLs. This magnitude is surprisingly homogeneous across the region under analysis, with slightly lower values over northern Africa. However, the homogeneity is reduced when the more extreme precipitation days are considered: CI values jump to 40-60% for days exceeding P90, above 60% over some areas for days above P95, and to a large area with above 60% values in the case of P99. In this case, a few sectors over eastern Spain and southern Italy reach values above 80%, meaning that 80% or more of the days in which precipitation exceeded P99 over those regions along the 1960-2014 period were associated with COLs.

b. COL-precipitation association in CMIP6 (low-resolution) models

Histograms of daily precipitation over the Mediterranean region built from historical CMIP6 data (Fig. 3) are overall similar to the ones discussed in the previous section. Still, some models depict peculiar behaviors such as too low zero-precipitation frequency (EC-Earth; Fig. 3h) or higher frequency in the 1-5 mm bin than in the 0.1-1 mm bin (IITM-ESM and IPSL-CM6A-LR; Fig. 3j,l). For reference, the annual-mean precipitation field in these models in the historical period is included in the Appendix (Fig. A1).

The spatial fields of COL frequencies in CMIP6 models (Fig. 4), in turn, show larger departures relative to ERA5. Indeed, most of the models depict a noticeable underestimation in the frequency of COLs over the Mediterranean and more markedly over the WMed box. At the same time, most of the models underestimate COL activity over the eastern Mediterranean and place the EMed maximum to the south of its location in reanalysis (cf. Fig. 1a). In fact, some of the models have this absolute maximum covering parts of northeastern Africa, where in turn ERA5 depicts values of less than 6 events per year. Area-weighted root-mean square error relative to ERA5 range between 22.70 and 39.48, with a multi-model mean of 28.98.

The contribution of COLs to annual precipitation and to extreme rainy days in CMIP6 models are shown in Fig. A2. When all rainy days are considered together, the pattern is similar to that derived from ERA5 data: the southern part of the study domain, mostly covering northern Africa, shows CI values of up to 20%. These values increase to the 20-40% range over the area north of 35ºN. However, in the case of CI computed for P99 (Fig. A3), the CMIP6 patterns are very different to that of the reanalysis: in fact, all the models maintain the entire Mediterranean region with CI magnitudes under 40%, having a large resemblance to the CI pattern for all rainy days taken together. Mathematically, this means that variations in the numerator (the number of days exceeding P99 when a COL is present) are similar to those in the denominator (the number of days exceeding P99 with or without a nearby COL). Physically, this means that the balance between COL-related and COL-unrelated precipitation events is the same for regular rainy days than for HPEs, unlike ERA5 in which HPEs become clearly dominated by a higher frequency of COL-driven precipitation. This is also supported by the larger area-weighted root mean square error values in P99 relative to all rainy days.

c. COL-precipitation association in EERIE (high-resolution) models

In this section we address whether eddy-rich models have a better representation of COL frequencies and the COL-precipitation linkages in comparison to the CMIP6 ensemble. We start by showing in Fig. 5 (left column) the annual-mean precipitation fields for the four high-resolution models, as well

https://doi.org/10.5194/egusphere-2026-4187
Preprint. Discussion started: 7 August 2026

as for the low-resolution version of HadGEM. The spatial patterns are similar to those of ERA5 both in terms of placing of the minima/maxima as well as on their magnitudes. In the case of HadGEM, the comparison between its eddy-rich version (Fig. 5g) and its low-resolution version (Fig. 5i) provides evidence on the added value of resolution on precipitation, becoming more clear close to areas with complex topography such as northern Spain, the Alps, the Apennines and the Balkans, where HadGEM-LL clearly underestimates the amounts of annual precipitation. However, the spatial averages in both cases are similar overall: 596.1 mm in HadGEM-HH versus 574.7 mm in HadGEM-LL. Results for the three other EERIE models show higher mean precipitation values in ICON and lower values in IFS-FESOM and IFS-NEMO.

The associated histograms (Fig. 5, right column) show that IFS-FESOM, IFS-NEMO and HadGEM-HH have similar rainfall distributions to those in ERA5. However, in the case of ICON, the distribution is characterized by too many zero-precipitation days and no difference between frequencies of bins 0.1-1 mm and 1-5 mm. Indeed, and somewhat surprisingly, the histogram from the low resolution HadGEM-LL model is closer to ERA5 than the one from ICON. Consequently, these biases in the ICON model should be taken into consideration in the remainder of the study and indicate that the benefits of the high resolution are not universal across all models.

In terms of COL climatology, EERIE models (Fig. 6) perform better than CMIP6 models. First, the frequency maximum over WMed becomes better defined in EERIE outputs as magnitudes get closer to those from ERA5. Also, the maximum over CMed is better defined in most EERIE models, and the associated maximum over EMed is found further north than in CMIP6, in better agreement with ERA5. In terms of magnitudes, the frequencies over the three are underestimated in EERIE, but biases are smaller compared to CMIP6 models. Areal-weighted root mean square errors for EERIE models are lower than for CMIP6 ones, with a multi-model mean value across the four ER models of 18.19, a minimum of 16.72 in IFS-NEMO and a maximum of 19.62 in IFS-FESOM. A quantitative comparison across model datasets is included further down in the manuscript.

CI fields built from historical EERIE data for all rainy days taken together and only for those exceeding P99 are shown in Fig. 7. In the case of the former, the simulated field is similar to that derived from both ERA5 and CMIP6 models, suggesting a negligible effect of horizontal resolution on this association. However, in the case of the HPEs, while ICON and IFS-FESOM are characterized by CI patterns similar to those considering all the rainy days, the other models (including the low-resolution version of HadGEM) show substantial improvements, with a marked increase in the contribution of COLs to extreme precipitation, much like the case of ERA5 and alike the CMIP6 models. Among all the EERIE models, the pattern that is closest to ERA5 is found in IFS-NEMO and HadGEM-HH as depicted by the lowest area-weighted root mean square errors.

d. Present and future of Mediterranean COLs in CMIP6 and EERIE models

Now we quantify the projected changes in COL frequency over the study area, focused on the three boxes with highest frequency. We do this for CMIP6 and EERIE models separately. As a reference, we show first in Fig. 8 the annual-mean frequency of COLs over the three boxes in ERA5, EERIE and CMIP6 models computed over the historical period 1960-2014. When compared to ERA5, all models underestimate the mean frequency of COLs in the three boxes (see the coloured dashed lines in the left y-axis of each plot, indicating the multi-model mean for EERIE and CMIP6 models in the top and bottom panels, respectively). However, the underestimation in EERIE is largely reduced compared to CMIP6, particularly over WMed and EMed. This is more clearly seen over WMed, with more than a

https://doi.org/10.5194/egusphere-2026-4187
Preprint. Discussion started: 7 August 2026

doubling of the CMIP6 frequency when EERIE models are considered, in closer agreement with ERA5. In turn, the simulated frequency over CMed is comparable between EERIE and CMIP6 models, suggesting a negligible impact of the increased resolution there.

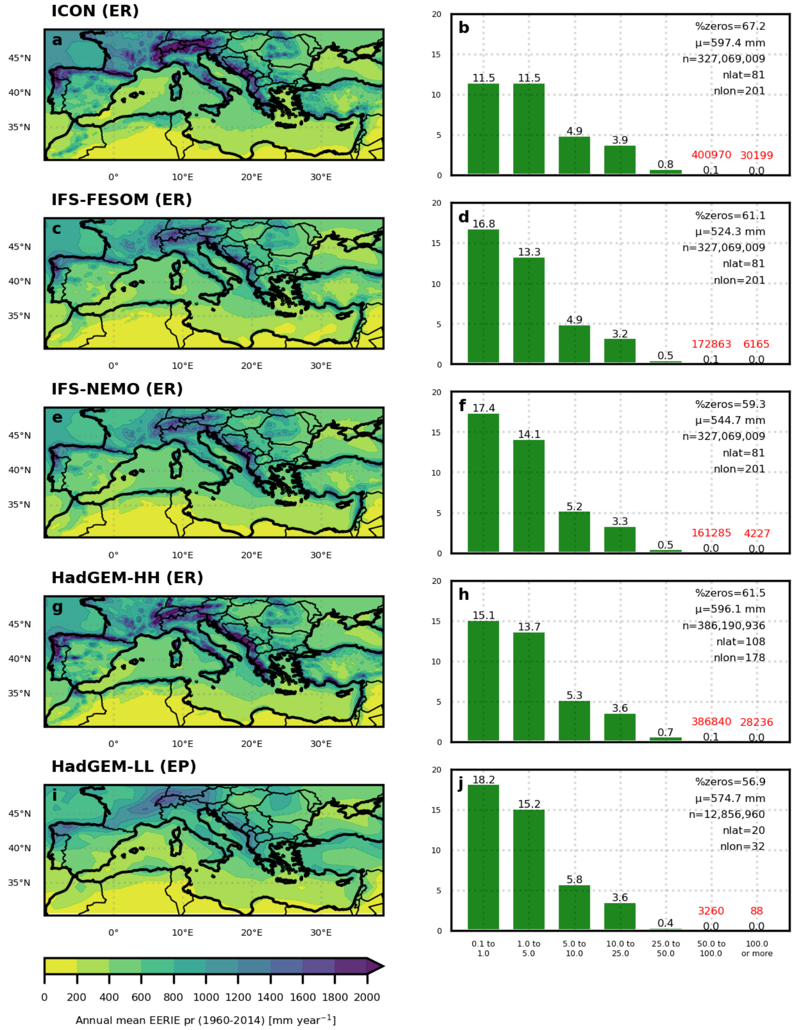

Figure 5 (left) Annual-mean precipitation (in mm year^{-1}), and (right) histograms of historical (1960-2014) daily precipitation over the Mediterranean region in EERIE models for the same bins considered in Figure 1b. The numbers in black above each bar indicate the percentage of values in that bin, while numbers in red above the two highest bins indicate the number of grid points included in these categories. Also shown in the upper right corner is the percentage of zero-precipitation values (i.e., precipitation amounts of less than 0.1 mm day^{-1}; %zeros), the spatial average of precipitation (μ), the total number of precipitation data (number of days x number of latitudes x number of longitudes; n), and the number of latitudes and longitudes (nlat and nlon, respectively) for each model.

https://doi.org/10.5194/egusphere-2026-4187
Preprint. Discussion started: 7 August 2026

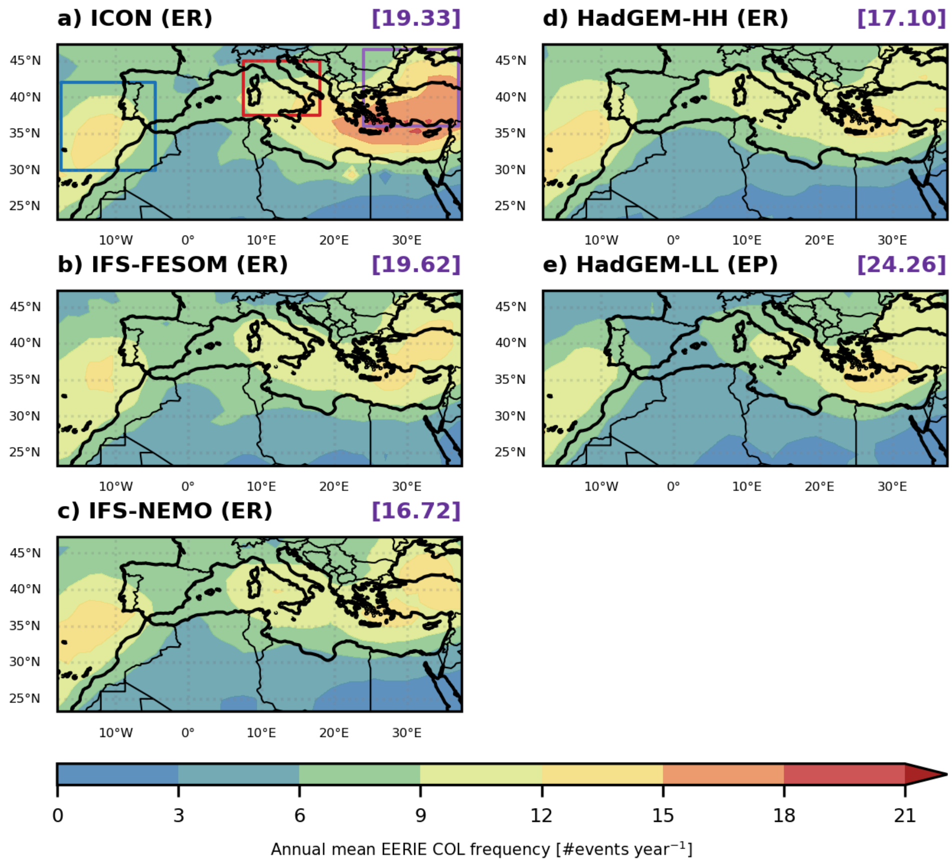

Figure 6 Annual mean frequency of COLs in EERIE models for the historical period (1960-2014) over the Mediterranean region. Values are expressed in number of events per year. For reference, the location of boxes WMed, CMed and EMed is displayed in panel a. The number in purple in each plot indicates the area-weighted root mean square error computed against ERA5.

https://doi.org/10.5194/egusphere-2026-4187
Preprint. Discussion started: 7 August 2026

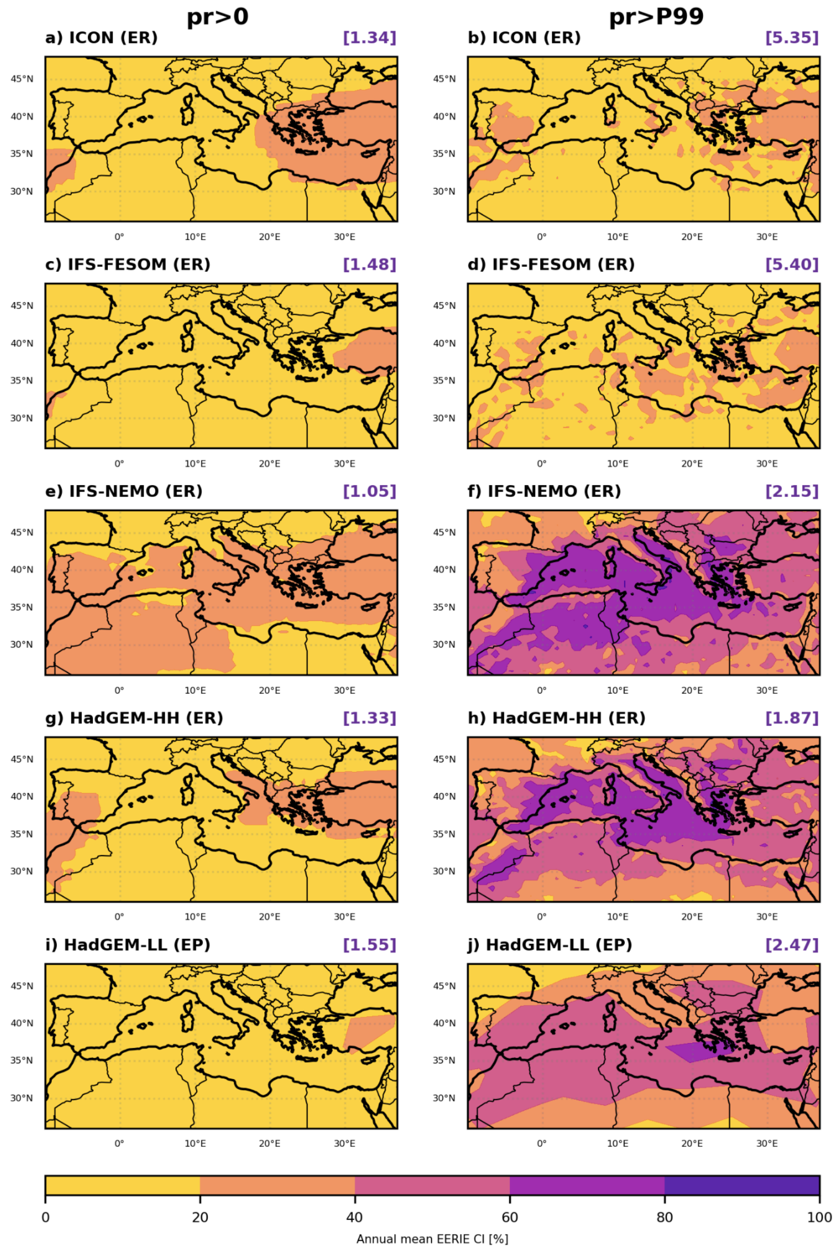

Figure 7 Spatial distribution of the annual CI in EERIE models (period 1960-2014) considering (left column) all days with non-zero precipitation, and (right column) days exceeding P99. Units are %. See text for further details. The number in purple in each plot indicates the area-weighted root mean square error computed against ERA5.

https://doi.org/10.5194/egusphere-2026-4187
Preprint. Discussion started: 7 August 2026

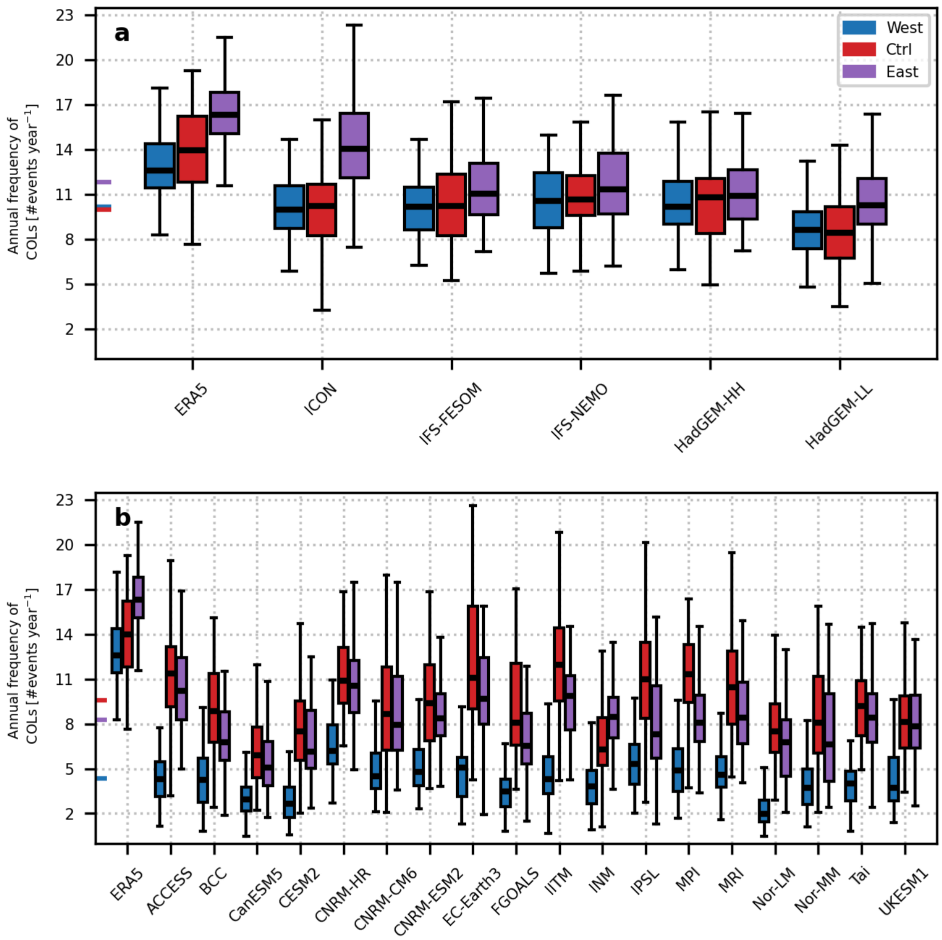

Figure 8 Boxplots of annual mean frequency of COLs averaged over the three boxes (WMed, CMed and EMed) in (a) EERIE models, and (b) CMIP models. Values for ERA5 are also included in both panels for reference. The three colored dashes on the left y-axis depict the multi-model mean for each box. Values are expressed in number of events per year.

https://doi.org/10.5194/egusphere-2026-4187
Preprint. Discussion started: 7 August 2026

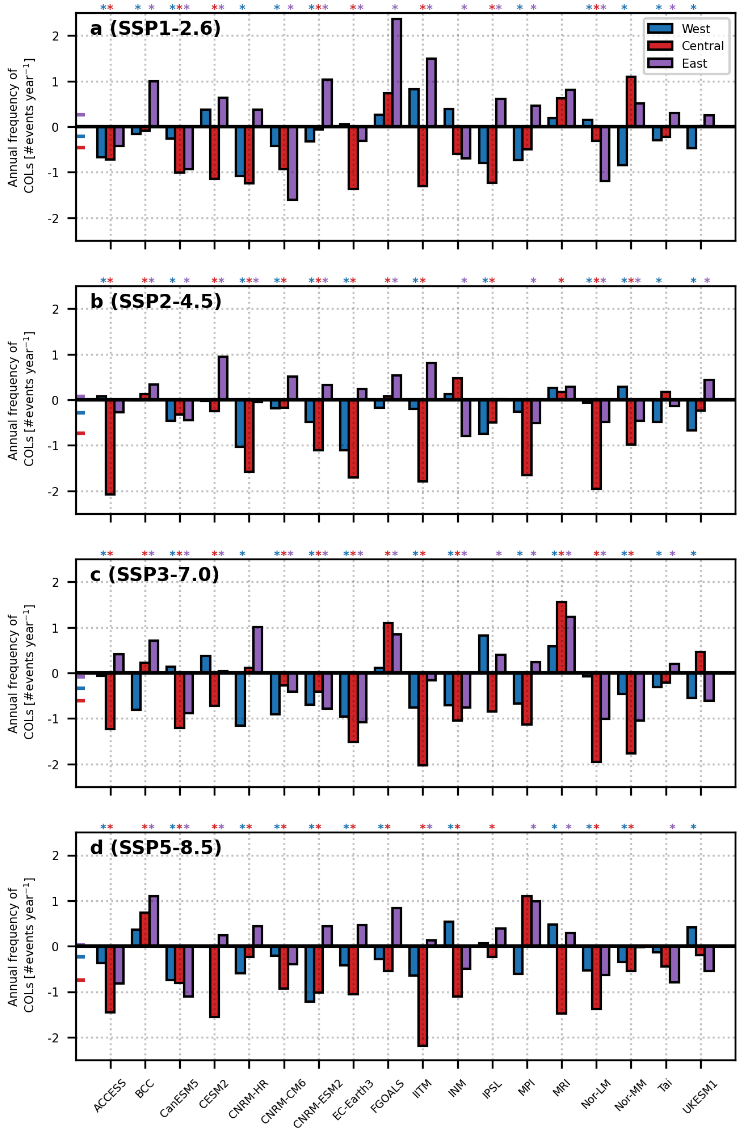

Figure 9 Differences in the annual-mean frequency of COLs in the future climate (2025-2050) relative to the historical conditions (1960-2014) for CMIP6 models averaged over the three boxes and as a function of the SSP: (a) SSP1-2.6, (b) SSP2-4.5, (c) SSP3-7.0, and (d) SSP5-8.5. The three colored dashes on the left y-axis depict the multi-model mean for each box. Values are expressed in number of events per year. Significant differences (p-val<0.05) are indicated with colored asterisks at the top of each panel using the same color convention.

https://doi.org/10.5194/egusphere-2026-4187
Preprint. Discussion started: 7 August 2026

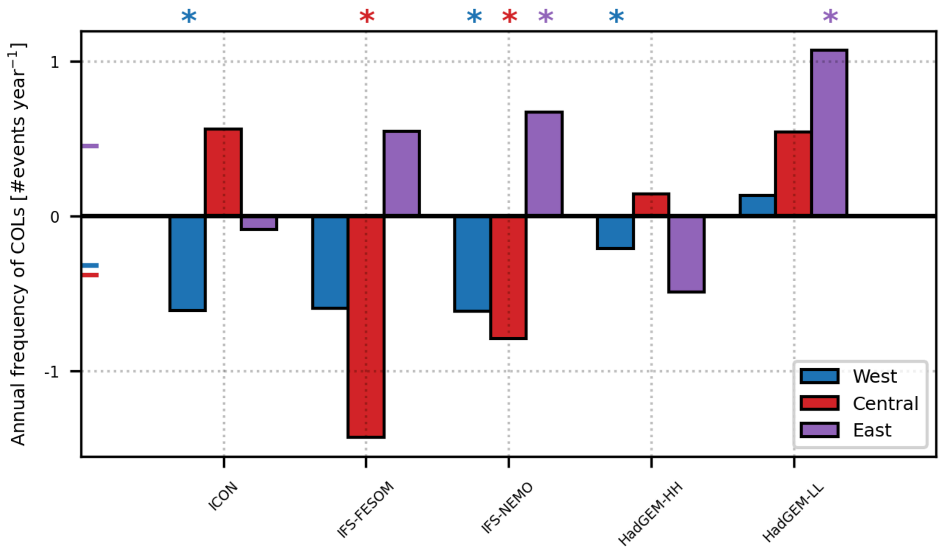

Figure 10 Differences in the annual-mean frequency of COLs in the future climate (2025-2050) relative to the historical conditions (1960-2014) for EERIE models averaged over the three boxes for the SSP considered in the EERIE project, SSP2-4.5. The three colored dashes on the left y-axis depict the multi-model mean for each box. Values are expressed in number of events per year. Significant differences (p-val<0.05) are indicated with colored asterisks at the top of each panel using the same color convention.

The spatial averages of the projected changes in Mediterranean COLs in CMIP6 and EERIE models are depicted in Fig. 9 and 10, respectively. In the case of CMIP6 (Fig. 9), substantial spread is found across both models and SSPs both in terms of magnitude and sign. Broadly, the multi-model means hint at reductions in the number of COLs over the WMed and CMed regions for the period 2025-2050 relative to 1960-2014 regardless of the SSP under consideration, while negligible changes are projected over the EMed region. Interestingly, the same patterns of variations are suggested by the EERIE models (Fig. 10), with a general reduction in the number of systems over WMed and CMed. Over EMed, these models do suggest a larger increase, but this result mostly comes from HadGEM-LL which does not benefit from the high resolution.

e. Dependence of the number of COLs on the horizontal resolution

In this section we further explore the relationship between the horizontal resolution used by the models and the number of COLs at each of the three boxes. To do so, we build scatterplots considering both metrics in each of the boxes (Fig. 11). For reference, we also show the associated values in ERA5 and NCEP-NCAR reanalyses. The first remarkable feature is the different behavior found in WMed and EMed compared to CMed: in the case of WMed and EMed, a clear improvement in the representation of COL frequencies with increasing resolution is evident. In fact, in both cases the four high-resolution EERIE models are above all CMIP6 models in terms of the number of systems, with a resulting clear negative slope in the linear fit and significant correlation coefficient values close to 0.6 (i.e., almost 40% of the variance in the number of COLs is explained by the horizontal resolution). On the other hand, while for the CMed we also see a generally improved

https://doi.org/10.5194/egusphere-2026-4187
Preprint. Discussion started: 7 August 2026

representation with increasing resolution, the linear relationship is less strong and several CMIP6 models represent more COLs — in line with ERA5 — than the EERIE models, with no clear distinction between the two groups. Another interesting feature results from the comparison of ERA5 and NCEP/NCAR with the model outputs. Even though EERIE models simulate COL frequencies closer to that in ERA5, none of the models reach the actual ERA5 value in any of the boxes under consideration. Furthermore, results for WMed suggest little dependence of resolution among EERIE models when analyzing their differences against ERA5, while in the case of CMed the most skillful model is the one having the largest horizontal resolution among the four models. In this case, the model using a comparable resolution to that of ERA5 is the one performing the worst. On the low-resolution side, results from the NCEP/NCAR reanalysis data are overall similar to those obtained from CMIP6 models, even though the reanalysis lies mostly above the models with comparable resolution.

f. Dependence of COL-related precipitation on the horizontal resolution

We explore next whether horizontal resolution has an impact on how models represent the magnitude of extreme precipitation associated with COLs. To do so, we first identify for each model (in both EERIE and CMIP6 datasets) the days with COLs at each of the three boxes, and for each of them we obtain the maximum precipitation (prmax) considering all grid points lying within 10 degrees to the east and 5 degrees north/south of the COL center as done in similar studies (Muñoz and Schultz, 2021). We then derive two metrics: one on the mean prmax computed over all the days in the historical period and a second one on the absolute maximum prmax across all days. The first metric measures the typical (mean) extreme precipitation associated with a COL, whereas the second one is the largest COL-related daily precipitation within the entire period of analysis.

We then build scatterplots for both metrics using all the available EERIE and CMIP6 models as well as ERA5 and NCEP/NCAR data. For simplicity, in this section we do not include EMed given that most of the precipitation associated with COLs lying in that area is located too far east of the study region and away from the Mediterranean region. The scatterplot built on the mean prmax value for each model and ERA5 (Fig. 12) shows once again a clear dependence on the horizontal resolution. Most of EERIE models lie above all the CMIP6 models and much closer to the value derived from ERA5 data. At the same time, and within the CMIP6 dataset, there is a substantial decrease in the magnitude of the mean prmax with decreasing resolution and the coarsest-resolution model (CanESM5) simulates a value that is between 1/6 and 1/10 those from the EERIE models. Across regions, little differences are found between WMed and CMed, with correlation coefficient values that are once again very close to one another (about -0.65). NCEP/NCAR values are once again comparable to outputs from low-resolution CMIP6 models.

When the highest precipitation associated with COLs is considered (i.e., the maximum of prmax), the resulting scatterplot (Fig. 13) becomes qualitatively similar to that described above for the mean value, but larger in terms of the associated magnitudes. This is reasonable, since now we are only considering the largest value of the 1960-2014 time series in each region. However, it is worth noting in this case that values simulated by EERIE models are not only larger to those from CMIP6, but also to those depicted in ERA5, with substantially larger magnitudes in both WMed and CMed. Part of the explanation for this might be the fact that EERIE models have larger resolution than ERA5, likely making them capable of representing precipitation extremes aided by the finer orography, like for example the one associated with the 2024 Valencia HPE. Again, correlation coefficients in both boxes

https://doi.org/10.5194/egusphere-2026-4187
Preprint. Discussion started: 7 August 2026

449 are significantly different from zero and indicate that more than 30% of the variance across models in
450 extreme precipitation is explained by horizontal resolution.

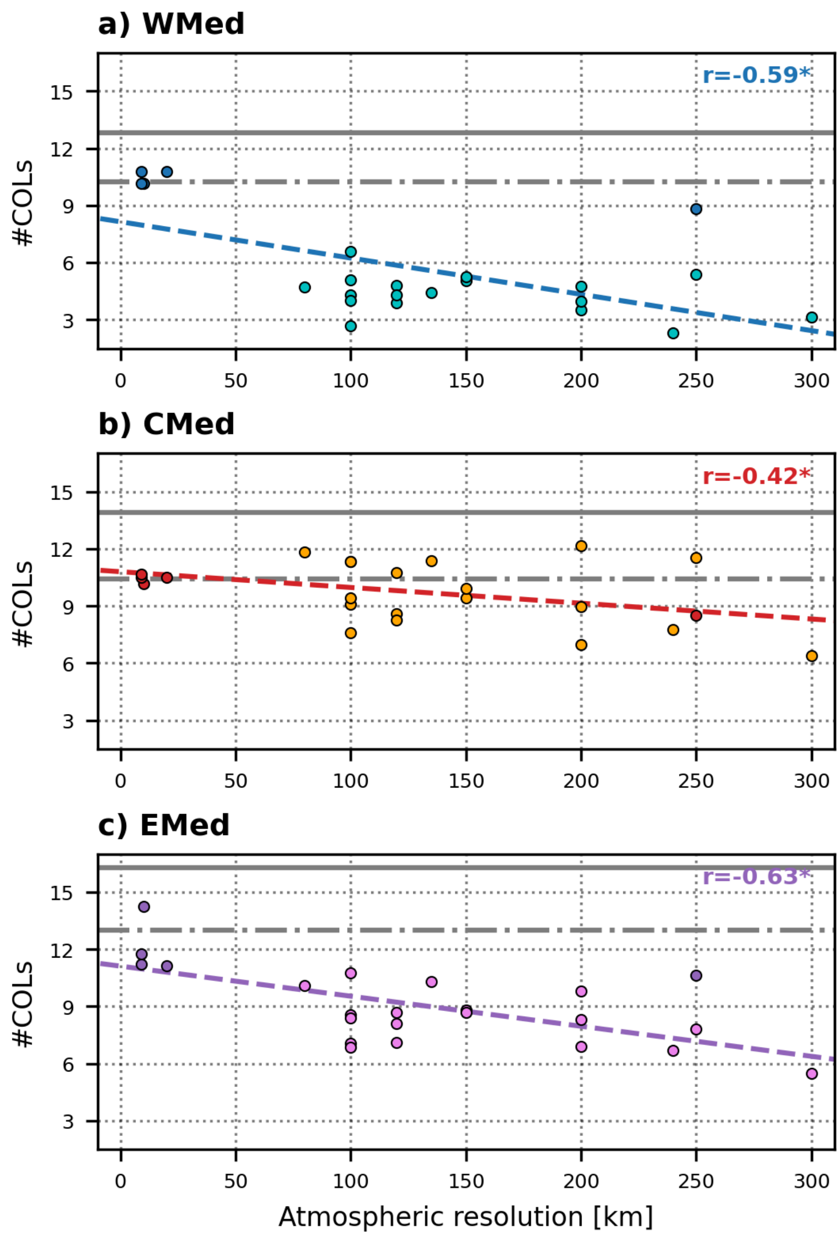

451

452 **Figure 11** Scatterplots between the horizontal atmospheric resolution (in km) and the annual frequency of COLs
453 in the historical conditions for EERIE (darker markers) and CMIP6 (lighter markers) in (a) WMed, (b) CMed,
454 and (c) EMed, along with the best linear fit and the value of the linear correlation coefficient. Significant
455 correlations (p-value<0.5) are highlighted with an asterisk. The full and dash-dotted lines in each panel show the
456 corresponding pair of values for the ERA5 and NCEP-NCAR datasets, respectively.

https://doi.org/10.5194/egusphere-2026-4187
Preprint. Discussion started: 7 August 2026

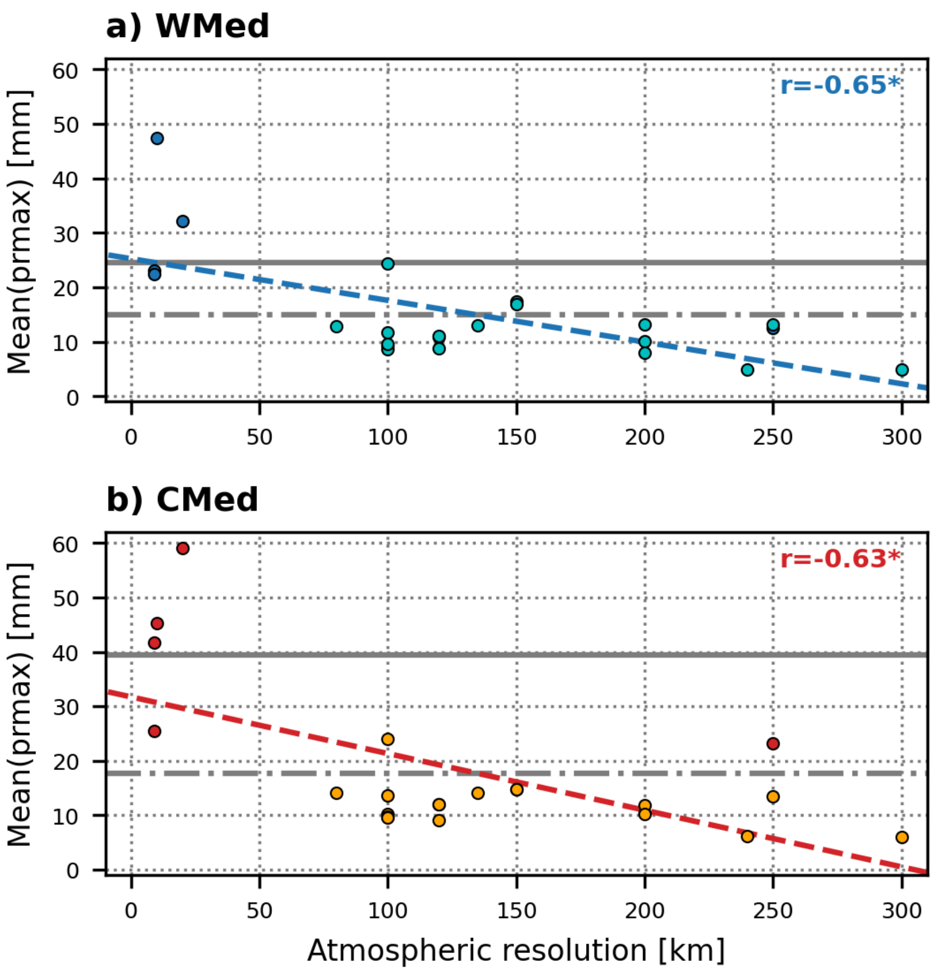

Figure 12 Scatterplots between the horizontal atmospheric resolution (in km) and the mean prmax value (in mm) in the historical conditions for EERIE (darker markers) and CMIP6 (lighter markers) models in (a) WMed, and (b) CMed, along with the best linear fit and the value of the linear correlation coefficient. Significant correlations (p-value<0.5) are highlighted with an asterisk. The full and dash-dotted lines in each panel show the corresponding pair of values for the ERA5 and NCEP-NCAR datasets, respectively. See text for further details.

https://doi.org/10.5194/egusphere-2026-4187
Preprint. Discussion started: 7 August 2026

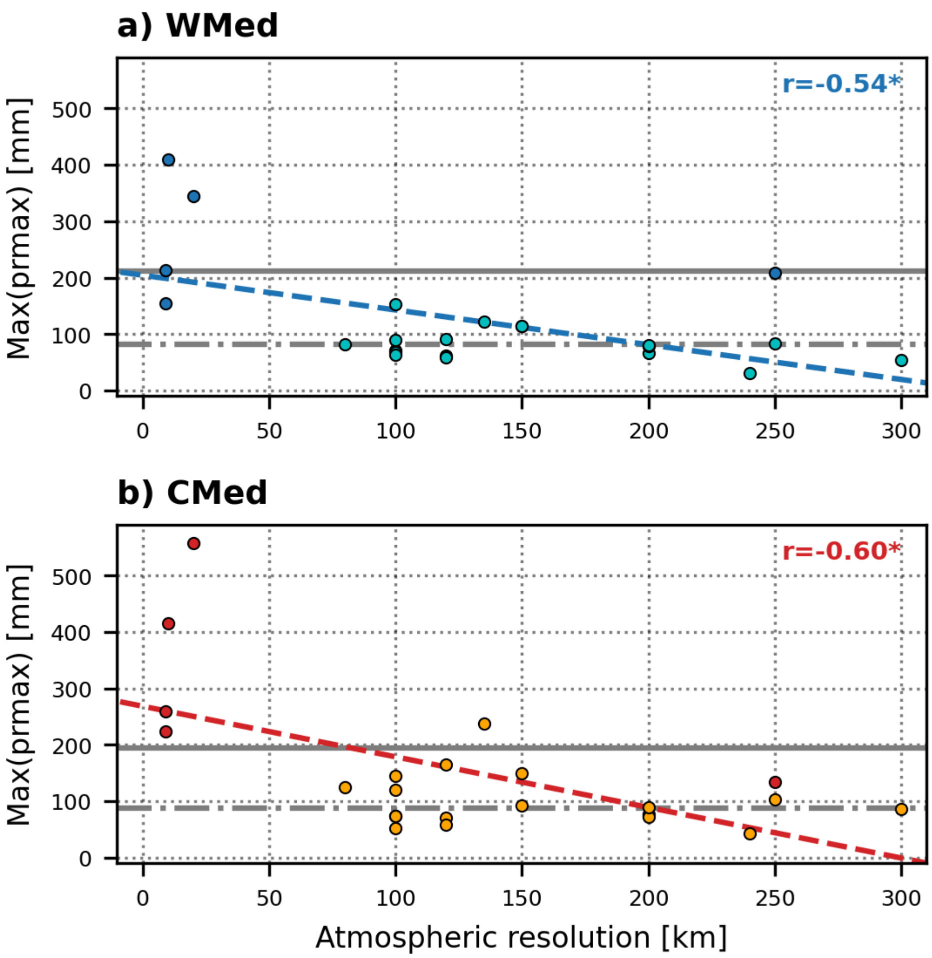

Figure 13 Scatterplots between the horizontal atmospheric resolution (in km) and the maximum prmax value (in mm) in the historical conditions for EERIE (darker markers) and CMIP6 (lighter markers) models in (a) WMed, and (b) CMed, along with the best linear fit and the value of the linear correlation coefficient. Significant correlations (p-value<0.5) are highlighted with an asterisk. The full and dash-dotted lines in each panel show the corresponding pair of values for the ERA5 and NCEP-NCAR datasets, respectively. See text for further details.

g. Future scenarios of extreme precipitation associated with COLs

We close this section by quantifying the projected changes in mean and maximum prmax associated with COLs in WMed and CMed for EERIE (one SSP) and CMIP6 (four SSPs) over the period 2025-2050 relative to 1960-2014. Results are shown as boxplots of the differences for all models in each dataset (n=4 for EERIE, as the low version of HadGEM is considered as a low-resolution model and therefore not included here, and n=18 for CMIP6) in Fig. 14. For reference, the boxplots built on the historical and future periods separately are shown in Fig. A4 and A5 in the Appendix, respectively.

https://doi.org/10.5194/egusphere-2026-4187
Preprint. Discussion started: 7 August 2026

In the case of the projected changes in the mean prmax (Fig. 14, top panel), results for EERIE and CMIP6 differ substantially. Over WMed (Fig. 14a), EERIE models hint at a slight reduction in mean prmax, with all models lying below the zero line and a multi-model median of -1.6 mm relative to historical conditions. By contrast, the majority of CMIP6 models project a slight increase in the mean prmax. This increase of the order of 1-2 mm is significantly different from the slight reduction indicated by the EERIE models (t-test, p-value<0.05). Results are even more different over CMed (Fig. 14c), as CMIP6 models project increases close to 3 mm in the metric while the signals of the EERIE models become more disparate. Indeed, the spread across EERIE models becomes substantially larger than that of CMIP6 models, in spite of the much smaller number of models. A similar feature is detected for the projected changes in maximum prmax over WMed (Fig. 14b), where once again EERIE models have the largest spread and even exceed that of all CMIP6 models in the four SSPs under consideration. The spread is reduced when the changes in maximum prmax over CMed are analyzed (Fig. 14d), but it still remains comparable to that of CMIP6 models in spite of the difference in the sample size. An inspection of the histograms built separately for historical and future conditions (Fig. S4,5) indicates that the larger spread across EERIE models is also detectable in each of the periods separately. Also, little dependence of the projections to the SSP selection is found for CMIP6 models for both historical and 2025-2050 climates.

4. Discussion and conclusions

The ability of modeling centers to perform very-high-resolution simulations of the climate system is rapidly increasing, leveraging the parallel increases in supercomputing power. These new experiments are expected not only to provide valuable information to understand and characterize the atmospheric processes and their influence on the regional climate but also to develop more trustworthy future climate scenarios. However, confronting evidence has so far emerged in studies on the role of this enhanced resolution on the representation of the oceanic and atmospheric circulation.

In this study we have analyzed the impact of very-high resolution on the formation of cut-off lows (COLs) over the Mediterranean Sea region and how these systems shape mean and extreme precipitation over southern Europe. COLs are a prominent feature of the regional climate and are frequently associated with heavy precipitation events (HPEs) and recent studies (e.g., Calvo-Sancho et al., 2026; Saurral et al., 2026) have pointed at a significant role of topography on the relationship of COLs and HPE due to its extra lifting mechanism.

We first computed the climatology of Mediterranean COLs in historical simulations of four eddy-rich (~10 km) models with comparable atmospheric resolution from the EERIE project and eighteen low-resolution models from CMIP6 and compared them against the ERA5 reanalysis. We found that even though most of the models underestimate the number of COLs over the region, the underestimation is reduced in the EERIE models, an evidence of a benefit stemming from high resolution which is particularly noticeable over the western Mediterranean sector. Then we looked at how COLs relate to precipitation events over southern Europe in reanalysis, CMIP6 and EERIE models. We found that CMIP6 models have a very poor representation of these linkages, particularly for upper-tail precipitation events (i.e., those exceeding percentiles 90, 95 and 99 of daily precipitation) where none of them capture the patterns depicted by the reanalysis. EERIE models perform better than CMIP6 overall, with most of the models showing a significant increase in the COL-precipitation relationship for the heavier rainfall events. However, a comparison among EERIE

https://doi.org/10.5194/egusphere-2026-4187
Preprint. Discussion started: 7 August 2026

models showed that two of them (ICON and IFS-FESOM) perform similarly to the CMIP6 models, which can be partly explained by the biases in the distribution of precipitation in these models. ICON, for instance, represents overall well the annual mean precipitation field but with too many zero-precipitation days relative to reanalysis. We also found that this model and IFS-FESOM both fail to capture the observed linkage between COLs and extreme precipitation over the Mediterranean.

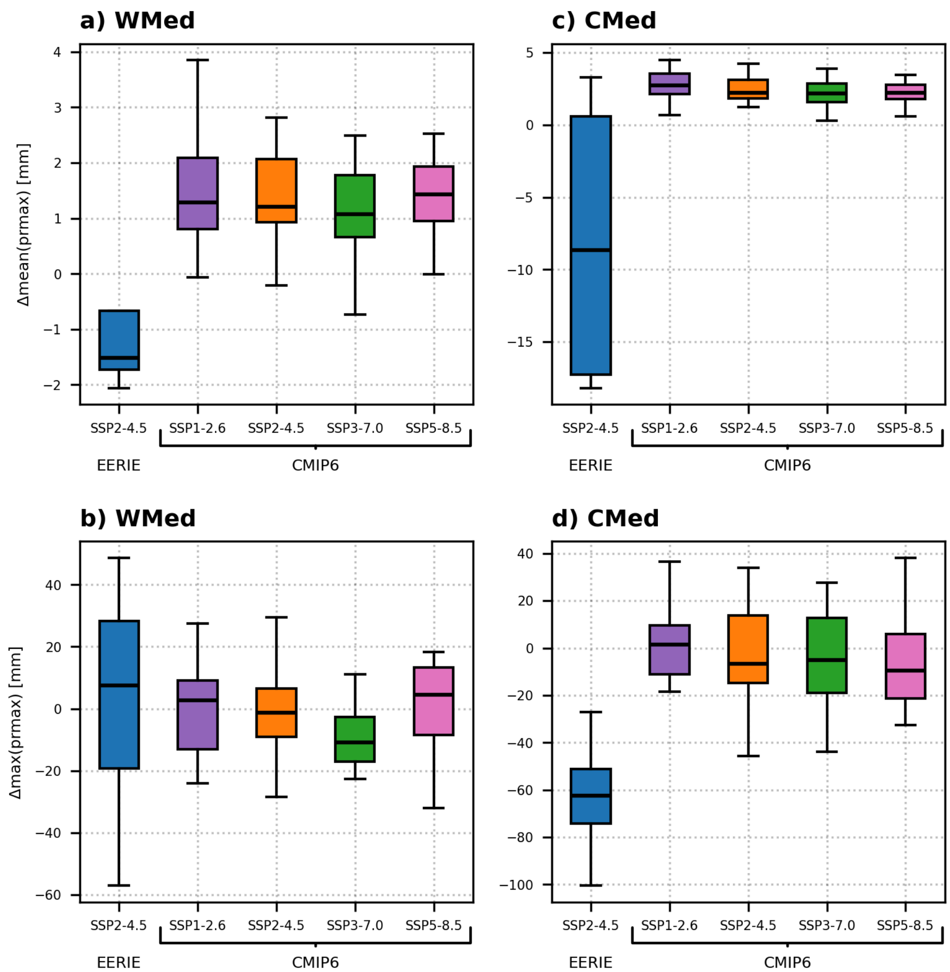

Figure 14 Boxplots of changes in (top) mean prmax, and (bottom) maximum prmax between the future and the historical climate, for EERIE models under SSP2-4.5 (blue bars) and CMIP6 models for (purple bars) SSP1-2.6, (orange bars) SSP2-4.5, (green bars) SSP3-7.0, and (pink bars) SSP5-8.5. Values are expressed in mm.

At the same time, we took the opportunity to compare one of the EERIE models (HadGEM-HH) with another simulation with the same model but carried out at low resolution (HadGEM-LL) and found that the lower-resolution version performs poorer than the high-resolution one but still better than some of the high-resolution EERIE models. This highlights the relative benefit of high resolution,

https://doi.org/10.5194/egusphere-2026-4187
Preprint. Discussion started: 7 August 2026

provided other sources of uncertainty such as how sub-scale processes are parameterized remain. In this regard, it is worth noting that the resolution adopted by the EERIE models is still insufficient for explicitly representing convective scale processes which can indeed be relevant in (COL-driven) HPEs.

Interestingly, when analyzing the projected changes in maximum precipitation amounts triggered by COLs over the Mediterranean region we found that EERIE models have a larger spread than CMIP6 models, even if their ensemble size is substantially smaller than the CMIP6 one (four models in the former dataset versus eighteen models in the latter). Therefore, even though very-high resolution is necessary to represent adequately the amounts of precipitation in COLs due, in part, to a better representation of topography (Saurral et al., 2026), the interplay between topography, COL location and local circulations that could likely emerge in the high-resolution experiments might lead to less uniform results. It is worth mentioning that convection-permitting simulations have been shown to have larger inter-model and inter-SSP spread in the projected changes in HPE properties relative to low-resolution experiments (e.g., Caillaud et al., 2024). Low-resolution models, on the other hand, have a significantly smoothed topography that makes this local-scale forcing less relevant in convective events.

Regarding the sign of the future changes in COL-precipitation relationship, we found that EERIE and CMIP6 models depict nearly opposite patterns: while EERIE models mostly suggest a future reduction in the intensity of extreme precipitation under COL events, CMIP6 models show an increase in its magnitude. Even though in this study we have not looked at the physical mechanisms responsible for such differences, this could be related to regional circulation changes responsible for the projected decrease in COLs. However, further research is needed to understand these uneven responses, which are of great relevance for the development of future rainfall scenarios over the Mediterranean Sea region, in particular considering the potentially devastating impacts of HPE over the area.

https://doi.org/10.5194/egusphere-2026-4187
Preprint. Discussion started: 7 August 2026

Appendix A

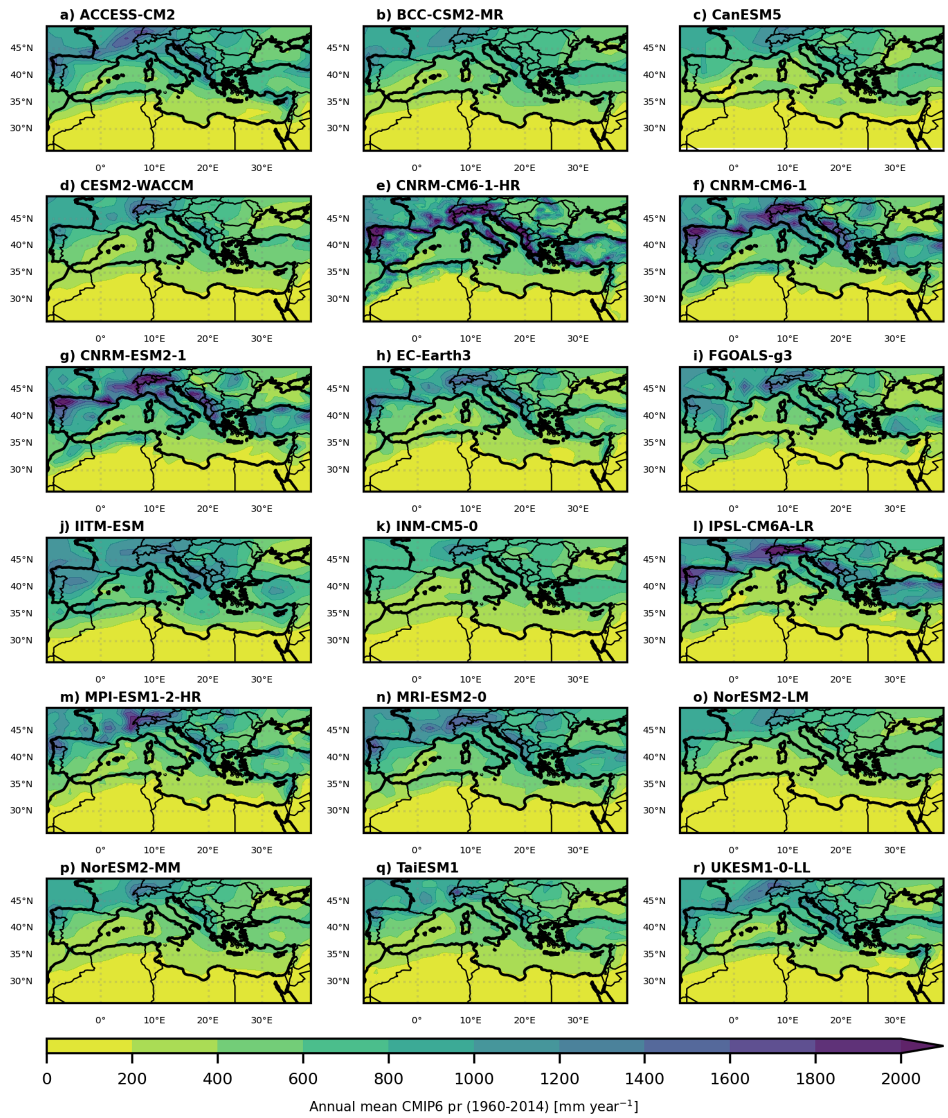

Figure A1 Annual-mean precipitation in CMIP6 models for the historical period, 1960-2014. Values are expressed in units of mm year^{-1}.

https://doi.org/10.5194/egusphere-2026-4187
Preprint. Discussion started: 7 August 2026

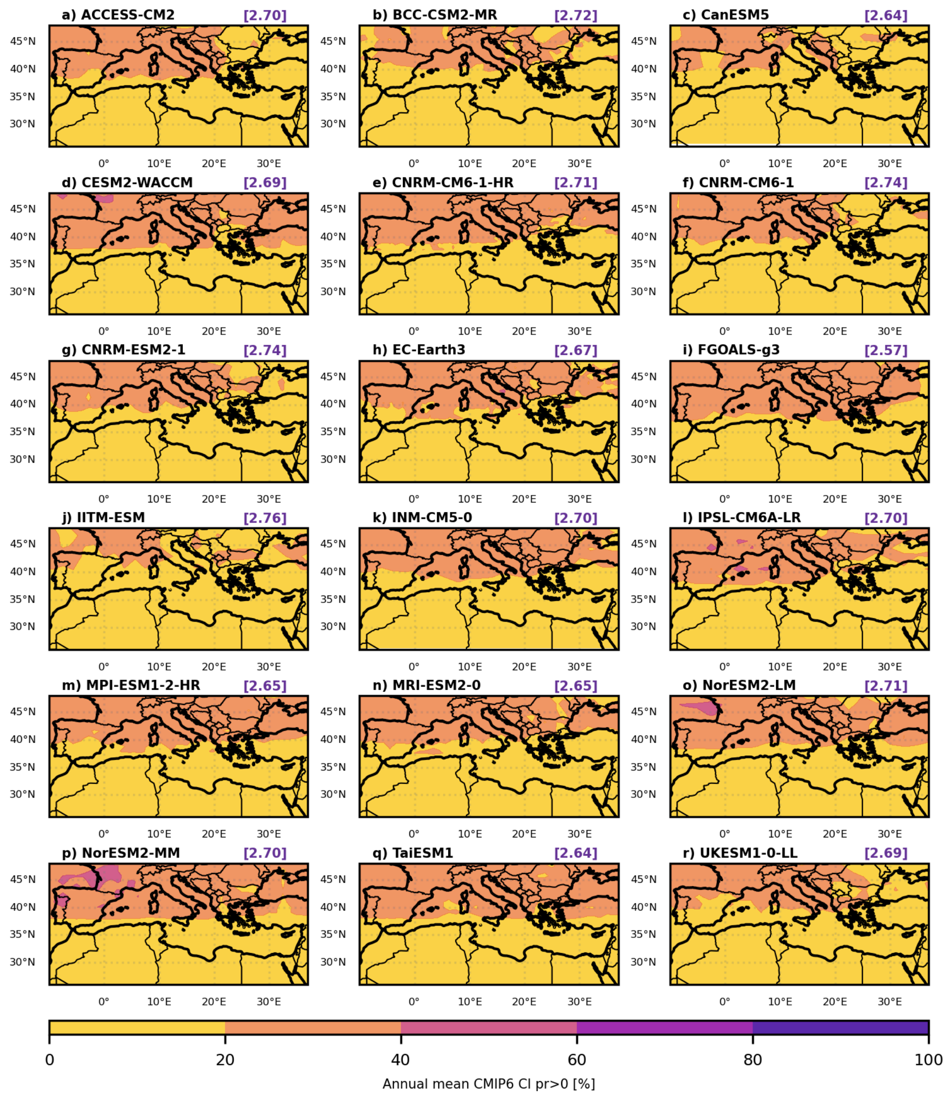

Figure A2 Spatial distribution of the annual CI considering all days with non-zero precipitation in CMIP6 models for the historical period, 1960-2014. Units are %. The number in purple in each plot indicates the area-weighted root mean square error computed against ERA5.

https://doi.org/10.5194/egusphere-2026-4187
Preprint. Discussion started: 7 August 2026

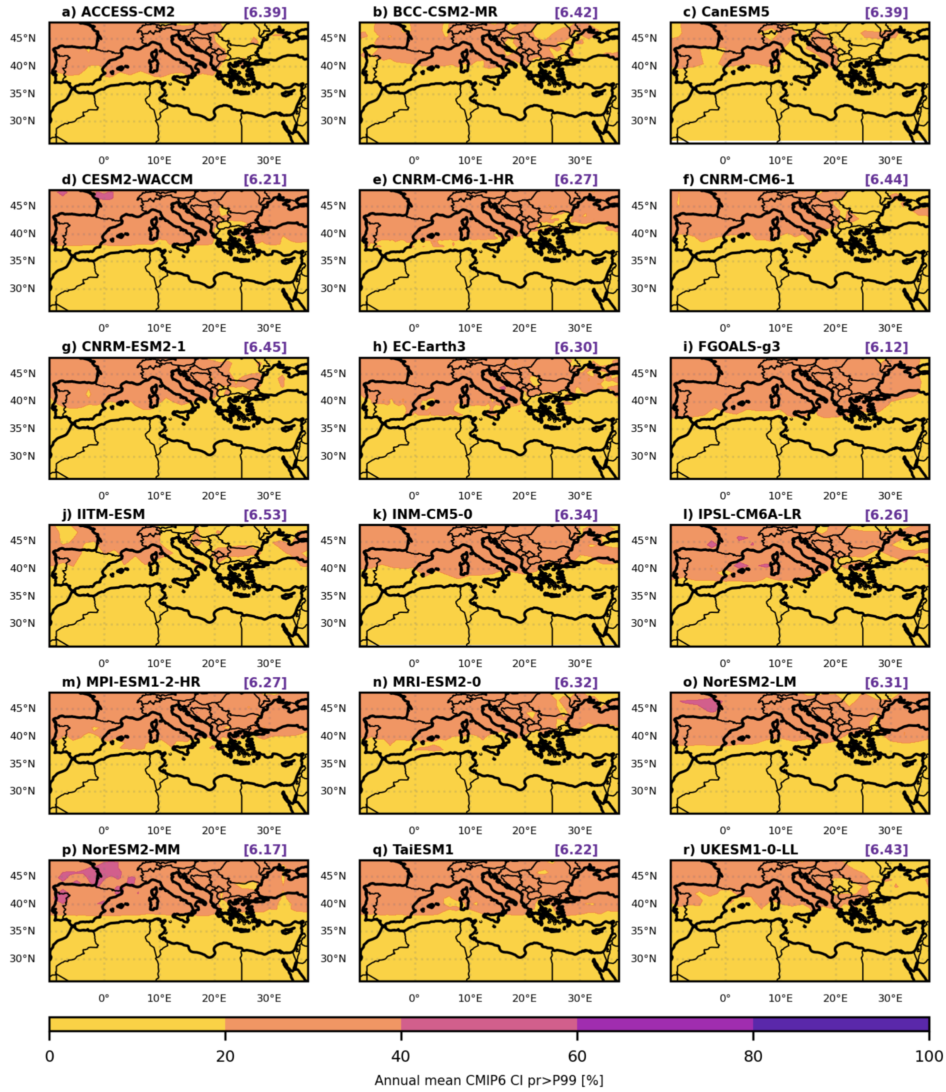

Figure A3 Spatial distribution of the annual CI considering days exceeding P99 in CMIP6 models for the historical period, 1960-2014. Units are %. The number in purple in each plot indicates the area-weighted root mean square error computed against ERA5.

https://doi.org/10.5194/egusphere-2026-4187
Preprint. Discussion started: 7 August 2026

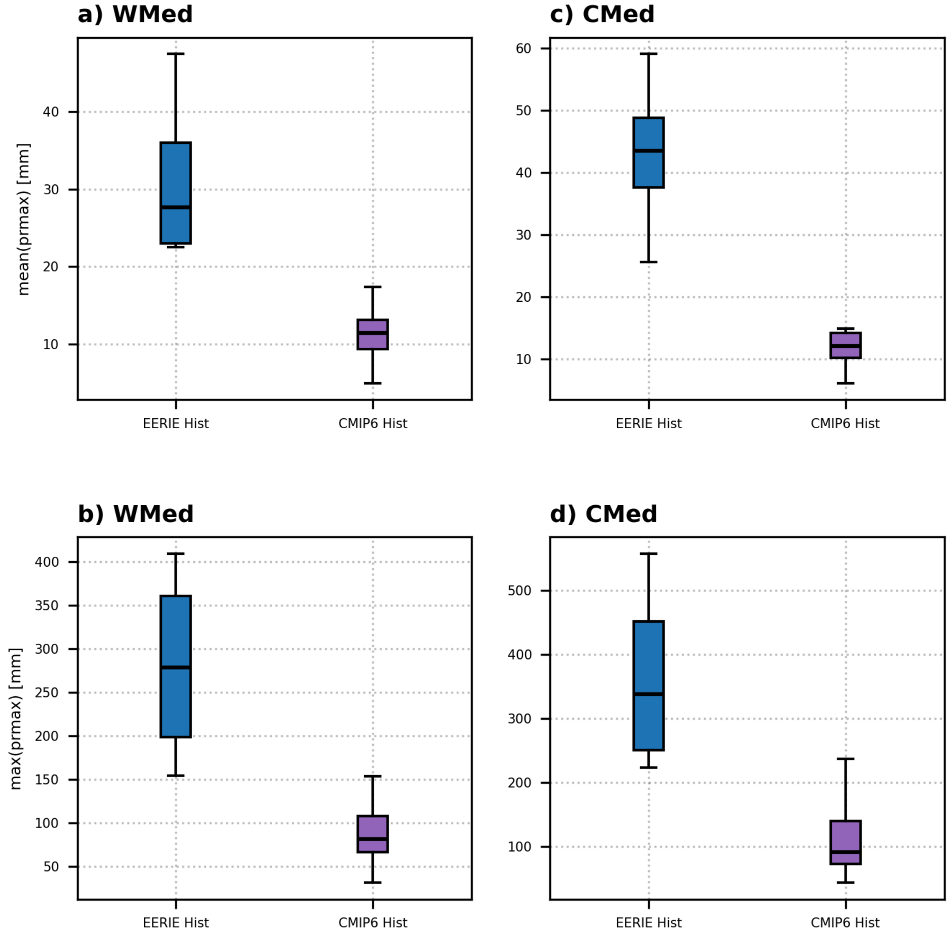

Figure A4 Boxplots of historical (top) mean prmax, and (bottom) maximum prmax for (blue bars) EERIE (purple bars) CMIP6 models. Values are expressed in mm.

https://doi.org/10.5194/egusphere-2026-4187
Preprint. Discussion started: 7 August 2026

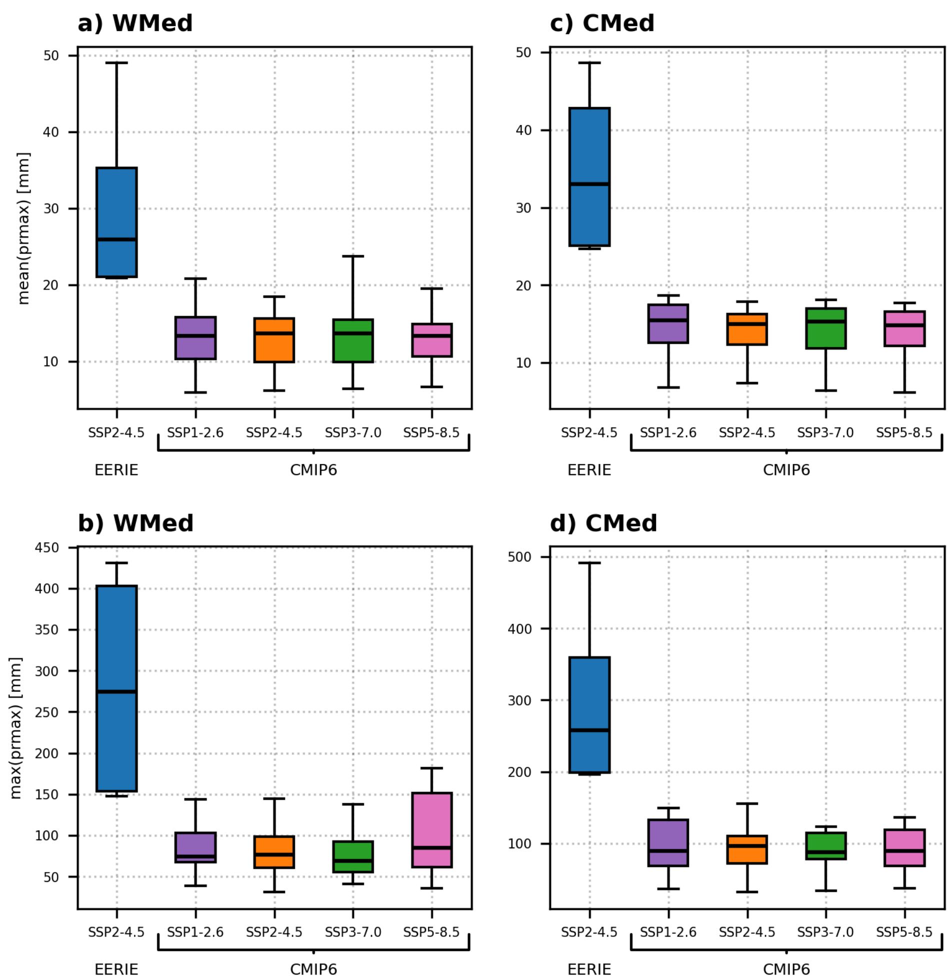

Figure A5 Boxplots of future (top) mean prmax, and (bottom) maximum prmax for (blue bars) EERIE models following the SSP2-4.5 scenario, and CMIP6 models following the (purple bars) SSP1-2.6, (orange bars) SSP2-4.5, (green bars) SSP3-7.0, and (pink bars) SSP5-8.5 scenarios. Values are expressed in mm.

Code availability

Scripts used to perform this study are available from the corresponding author on request.

Data availability statement

ERA5 reanalysis is available from the Copernicus Climate Change Service Climate Data Store (https://doi.org/10.24381/cds.bd0915c6). NCEP/NCAR Reanalysis I data is available at the National Oceanic and Atmospheric Administration (NOAA)'s Physical Sciences Laboratory website (https://psl.noaa.gov/data/gridded/data.ncep.reanalysis.html). EERIE data is available through the EERIE cloud data server developed by DKRZ

https://doi.org/10.5194/egusphere-2026-4187
Preprint. Discussion started: 7 August 2026

(https://swift.dkrz.de/v1/dkrz_7fa6baba-db43-4d12-a295-8e3ebb1a01ed/apps/stac-browser/index.html).

Author contribution

RS: conceptualization; data curation; formal analysis; investigation; methodology; software; supervision; visualization; writing (original draft).
AMP: formal analysis; investigation.
DC: formal analysis; investigation; writing (review and editing)
JJGA: formal analysis; investigation; writing (review and editing)
SLT: software
PO: formal analysis; funding acquisition; methodology; supervision; writing (review and editing)

Competing interests

The authors declare that they have no conflict of interest.

Acknowledgments

This publication is part of the EERIE project funded by the European Union (Grant Agreement No. 101081383). Views and opinions expressed are however those of the authors only and do not necessarily reflect those of the European Union or the European Climate Infrastructure and Environment Executive Agency (CINEA). Neither the European Union nor the granting authority can be held responsible for them. RS acknowledges his AI4S fellowship within the "Generación D" initiative by Res.es, Ministerio para la Transformación Digital y de la Función Pública of Spain, for talent attraction (C005/24-ED CV1), funded by NextGenerationEU through PRTR. The authors thank the modelling teams at AWI, BSC, Met Office and MPI for developing and making available the very-high resolution experiments used in this study.

Financial support

EERIE project funded by the European Union (Grant Agreement No. 101081383).

https://doi.org/10.5194/egusphere-2026-4187
Preprint. Discussion started: 7 August 2026

References

Bi, D., M. Dix, S. Marsland, S. O'Farrell, et al., 2020: Configuration and spin-up of ACCESS-CM2, the new generation Australian Community Climate and Earth System Simulator Coupled Model. J. South. Hem. Earth Sys. Sci., **70**, 225-251. https://doi.org/10.1071/ES19040.

Boucher, O., J. Servonnat, A. Albright, O. Aumont, Y. Balkanski, et al., 2020: Presentation and evaluation of the IPSL-CM6A-LR climate model. J. Adv. Mod. Earth Sys., **12**, e2019MS

Caillaud, C., S. Somot, H. Douville, A. Alias, S. Bastin, S. Brienen, et al., 2024: Northwestern Mediterranean heavy precipitation events in a warmer climate: Robust versus uncertain changes with a large convection-permitting model ensemble. Geophys. Res. Lett., **51**, e2023GL105143. https://doi.org/10.1029/2023GL105143.

Calvo-Sancho, C., J. Díaz-Fernández, J. González-Alemán, A. Halifa-Marín, M. Miglietta, C. Azorin-Molina, A. Prein, A. Montoro-Mendoza, P. Bolgiani, A. Morata, and M. Martín, 2025: Human-induced climate change amplification on storm dynamics in Valencia's 2024 catastrophic flash flood. Nat. Commun., **17**, 1492. https://doi.org/10.1038/s41467-026-68929-9.

Campos, D., M. Olmo, P. Cos, A. Muñoz, and F. Doblas-Reyes, 2025: Regional aspects of observed temperature and precipitation trends in the western Mediterranean: insights from a timescale decomposition analysis. J. Geophys. Res.: Atmos., **130**, e2024JD042637. https://doi.org/10.1029/2024JD042637.

Campos, D., K. Grayson, R. Saurral, S. Beyer, A. John, M. Olmo, and F. Doblas-Reyes, 2026: The October 2024 extreme precipitation event over Valencia: storyline attribution of the synoptic-scale thermodynamic drivers. Wea. Clim. Dyn., **7**, 1153-1171. https://doi.org/10.5194/wcd-7-1153-2026.

Chen, T.-C., H. Goosse, C. Davrinche, S. Libera, C. Roberts, M. Aengenheyster, K. Strommen, M. Roberts, R. Ghosh, and J.-S. von Storch, 2025; Southern Annular Mode persistence and westerly jet: a reassessment using high-resolution global models. Wea. Cli. Dyn., 6, 1179-1193. https://doi.org/10.5194/wcd-6-1179-2025.

Chericoni, M., G. Fosser, E. Flaounas, M. Gaetani, and A. Anav, 2025: Unravelling drivers of the future Mediterranean precipitation paradox during cyclones. npj Clim Atmos Sci, **8**, 260. https://doi.org/10.1038/s41612-025-01121-w.

Choquehuanca, B., A., Godoy, and R. Saurral, 2025: Assessing the skill of high-impact weather forecasts in southern South America: a study on cut-off lows. Wea. Cli. Dyn., **6**, 317–327. https://doi.org/10.5194/egusphere-2024-1063.

Cornes, R., G. van der Schrier, E. van den Besselaar, and P. Jones, 2018: An ensemble version of the E-OBS temperature and precipitation datasets. J. Geophys. Res. Atmos., **123**, 9391–9409. https://doi.org/10.1029/2017JD028200.

Cos, J., F. Doblas-Reyes, M. Jury, R. Marcos, P.-A. Bretonnière, and M. Samsó, 2022: The Mediterranean climate change hotspot in the CMIP5 and CMIP6 projections. Earth Sys. Dyn., **13**, 321-340. https://doi.org/10.5194/esd-13-321-2022.

Danabasoglu, G., J.-F. Lamarque, J. Bacmeister, D. Bailey, et al., 2020: The Community Earth System Model version 2 (CESM2). J. Adv. Mod. Earth Sys., **12**, e2019MS001916. https://doi.org/10.1029/2019MS001916.

Dhame, S., D. Olonscheck, and M. Rugenstein, 2025: Higher-resolution climate models do not consistently reproduce the observed Tropical Pacific warming pattern. J. Climate, **38**, 3131-3149. https://doi.org/10.1175/JCLI-D-24-0248.1.

Doblas-Reyes, F., J. Kontkanen, I. Sandu, M. Acosta, et al., 2026: The Destination Earth digital twin for climate change adaptation. Geosci. Mod. Dev., **19**, 2821-2848. https://doi.org/10.5194/gmd-19-2821-2026.

https://doi.org/10.5194/egusphere-2026-4187
Preprint. Discussion started: 7 August 2026

Döscher, R., M. Acosta, A. Alessandri, P. Anthoni, T. Arsouze, et al., 2022: The EC-Earth3 Earth system model for the Coupled Model Intercomparison Project 6. Geosci. Mod. Dev., **15**, 2973-3020. https://doi.org/10.5194/gmd-15-2973-2022.

Favre, A., B. Hewitson, C. Lennard, R. Cerezo-Mota, and M. Tadross, 2013: Cut-off lows in the South Africa region and their contribution to precipitation. Clim. Dyn., **41**, 2331-2351. https://doi.org/10.1007/s00382-012-1579-6.

Giorgi, F., 2006: Climate change hot-spots. Geophys. Res. Lett., L08707. https://doi.org/10.1029/2006GL025734.

Hersbach, H., Bell, B., Berrisford, P., and coauthors, 2020: The ERA5 global reanalysis. Quart. J. Roy. Met. Soc., **146**, 1999-2049. https://doi.org/10.1002/qj.3803.

Hohenegger, C., P. Korn, L. Linardakis, R. Redler, R. Schnur, and coauthors, 2023: ICON-Sapphire: simulating the components of the Earth system and their interactions at kilometer and subkilometer scales. Geosci. Mod. Dev., **16**, 779-811. https://doi.org/10.5194/gmd-16-779-2023.

Iles, C., R. Vautard, J. Strachan, S. Joussaume, B. Eggen, and C. Hewitt, 2020: The benefits of increasing resolution in global and regional climate simulations for European climate extremes. Geosci. Mod. Dev., **13**, 5583-5607. https://doi.org/10.5194/gmd-13-5583-2020.

Insua-Costa, D., M. Senande-Rivera, M. C. Llasat, and G. Miguez-Macho, 2022: A global perspective on western Mediterranean precipitation extremes. npj Clim. Atmos. Sci., **5**, 9. https://doi.org/10.1038/s41612-022-00234-w.

John, A., S. Beyer, M. Athanase, A. Sánchez-Benítez, H. Goessling, A. Hossain, et al., 2026: Global kilometer-scale climate storylines using spectral nudging. J. Adv. Mod. Earth Sys., 18, e2025MS005326. https://doi.org/10.1029/2025MS005326.

Jury, M., 2024: Statistics and meteorology of cutoff lows over South Africa 1970-2023. Climate, **12**, 152. https://doi.org/10.3390/cli12100152.

Kalnay, E., M. Kanamitsu, R. Kistler, W. Collins, D. Deaven, et al., 1996: The NCEP/NCAR 40-year reanalysis project. Bull. Amer. Meteor. Soc., **77**, 437-471. https://doi.org/10.1175/1520-0477(1996)077<0437:TNYRP>2.0.CO;2.

Kasuga, S., and M. Honda, 2025: Climatology of cutoff lows approaching Japan. SOLA, 2025-049. https://doi.org/10.2151/sola.2025-049.

Kasuga, S., M. Honda, J. Ukita, S. Yamane, H. Kawase, and A. Yamazaki, 2021: Seamless detection of cutoff lows and preexisting troughs. Mon. Wea. Rev., **149**, 3119-3134. https://doi.org/10.1175/MWR-D-20-0255.1.

Lee, W.-L., Y.-C. Wang, C.-J. Shiu, I.-C. Tsai, et al., 2020: Taiwan Earth System Model version 1: description and evaluation of mean state. Geosci. Mod. Dev., **13**, 3887-3904. https://doi.org/10.5194/gmd-13-3887-2020.

Li, L., Y. Yu, P. Lin, J. Xie, M. Song, L. Dong, et al., 2020: The Flexible Global Ocean-Atmosphere-Land System Model Grid-Point Version 3 (FGOALS-g3): Description and evaluation. J. Adv. Mod. Earth Sys., **12**, e2019MS002012. https://doi.org/10.1029/2019MS002012.

Lionello, P., and L. Scarascia, 2018: The relation between climate change in the Mediterranean region and global warming. Reg. Environm. Change, **18**, 1481-1493. https://doi.org/10.1007/s10113-018-1290-1.

Lupo, K., C. Schwartz, and G. Romine, 2023: Displacement error characteristics of 500-hPa cutoff lows in operational GFS forecasts. Wea. Forecasting, **38**, 1849-1871. https://doi.org/10.1175/WAF-D-22-0224.1.

Mastrantonas, N., P. Herrera-Lormendez, L. Magnusson, F. Pappenberger, and J. Matschullat, 2021: Extreme precipitation events in the Mediterranean: spatiotemporal characteristics and connection to large-scale atmospheric flow patterns. Int. J. Climatol., **41**, 2710-2728. https://doi.org/10.1002/joc.6985.

https://doi.org/10.5194/egusphere-2026-4187
Preprint. Discussion started: 7 August 2026

Moreno-Chamarro, E., L.-P. Caron, P. Ortega, S. Loosveldt Tomas, and M. Roberts, 2021: Can we trust CMIP5/6 future projections of European winter precipitation? Environ. Res. Lett., **16**, 054063. https://doi.org/10.1088/1748-9326/abf28a.
Müller, S., E. Pichelli, E. Coppola, et al., 2024: The climate change response of alpine-Mediterranean heavy precipitation events. Clim. Dyn., **62**, 165-186. https://doi.org/10.1007/s00382-023-06901-9.
Müller, W., J. Jungclaus, T. Mauritsen, J. Baehr, et al., 2018: A higher-resolution version of the Max Planck Institute Earth System Model (MPI-ESM1.2-HR). J. Adv. Mod. Earth Sys., **10**, 1383-1413. https://doi.org/10.1029/2017MS001217.
Muñoz, C., and D. Schultz, 2021: Cutoff lows, moisture plumes, and their influence on extreme-precipitation days in central Chile. J. Appl. Meteor. Climatol., **60**, 437-454. https://doi.org/10.1175/JAMC-D-20-0135.1.
Nellikkattil, A., J. Lee, B. Guan, A. Timmermann, S. Lee, J. Chu, and D. Lemmon, 2023: Increased amplitude of atmospheric rivers and associated extreme precipitation in ultra-high-resolution greenhouse warming simulations. Commun. Earth Env., **4**, 313. https://doi.org/10.1038/s43247-023-00963-7.
Nieto, R., L. Gimeno, L. de la Torre, P. Ribera, D. Gallego, R. García-Herrera, J. García, M. Núñez, A. Redaño, and J. Lorente, 2005: Climatological features of cutoff low systems in the Northern Hemisphere. J. Clim., **18**, 3085-3103. https://doi.org/10.1175/JCLI3386.1.
Palmen, E., and C. Newton, 1969: Atmospheric circulation systems. Academic Press, New York, 471-522.
Pinheiro, H., T. Ambrizzi, K. Hodges, M. Gan, K. Andrade, and J. García, 2022: Are cut-off lows simulated better in CMIP6 compared to CMIP5? Clim. Dyn., **59**, 2117-2136. https://doi.org/10.1007/s00382-022-06200-9.
Porcù, F., A. Carrassi, C. Medaglia, F. Prodi, and A. Mugnai, 2007: A study on cut-off low vertical structure and precipitation in the Mediterranean region. Meteor. Atmos. Phys., **96**, 121-140. https://doi.org/10.1007/s00703-006-0224-5.
Prein, A., W. Langhans, G. Fosser, A. Ferrone, N. Ban, et al., 2015: A review on regional convection-permitting climate modeling: demonstrations, prospects, and challenges. Rev. Geophys., **53**, 323-361. https://doi.org/10.1002/2014RG000475.
Price, J., and G. Vaughan, 1992: Statistical studies of cut-off low systems. Ann. Geophys., **10**, 96-102.
Rackow, T., X. Pedruzo-Bagazgoitia, T. Becker, S. Milinski, et al., 2025: Multi-year simulations at kilometre scale with the Integrated Forecasting System coupled to FESOM2.5 and NEMOv3.4. Geosci. Mod. Dev., **18**, 33-69. https://doi.org/10.5194/gmd-18-33-2025.
Ramonell, D., D. Carrió, A. Amengual, and R. Romero, 2026: Assessing high-resolution numerical models and bottom-boundary factors for a Mediterranean heavy precipitation event. Quart. J. Royal Met. Soc., e70132. https://doi.org/10.1002/qj.70132.
Reale, M., W. Cabos Narvaez, L. Cavicchia, et al., 2022: Future projections of Mediterranean cyclone characteristics using the Med-CORDEX ensemble of coupled regional climate system models. Clim. Dyn., **58**, 2501–2524. https://doi.org/10.1007/s00382-021-06018-x.
Reder, A., M. Raffa, R. Padulano, G. Rianna, and P. Mercogliano, 2022: Characterizing extreme values of precipitation at very high resolution: an experiment over twenty European cities. Wea. Cli. Extr., **35**, 100407. https://doi.org/10.1016/j.wace.2022.100407.
Roberts, M., K. Reed, Q. Bao, J. Barsugli, S. Camargo, et al., 2025: High-Resolution Model Intercomparison Project phase 2 (HighResMIP2) towards CMIP7. Geosci. Mod. Dev., **18**, 1307-1332. https://doi.org/10.5194/gmd-18-1307-2025.
Saurral, R., D. Campos, K. Grayson, V. Lapin, P. Trascasa Castro, E. Tourigny, S. Materia, E. Ferrer, and F. Doblas-Reyes, 2026: The key role of Mediterranean and North Atlantic sea surface

https://doi.org/10.5194/egusphere-2026-4187
Preprint. Discussion started: 7 August 2026

temperatures on the 2024 record-breaking Valencia precipitation event. Wea. Cli. Extr., **52**, 100877. https://doi.org/10.1016/j.wace.2026.100877.

Saurral, R., F. Doblas-Reyes, J. Screen, J. Catto, S. Hay, and H. Yu, 2025: Western Mediterranean droughts fostered by Arctic sea ice loss. J. Clim., **38**, 3005-3014. https://doi.org/10.1175/JCLI-D-25-0066.1.

Séférian, R., P. Nabat, M. Michou, D. Saint-Martin, A. Voldoire, et al., 2019: Evaluation of CNRM Earth System Model, CNRM-ESM2-1: Role of Earth System processes in present-day and future climate. J. Adv. Mod. Earth Sys., **11**, 4182-4227. https://doi.org/10.1029/2019MS001791.

Seland, Ø., M. Bentsen, D. Olivié, T. Toniazzo, et al., 2020: Overview of the Norwegian Earth System Model (NorESM2) and key climate response of CMIP6 DECK, historical, and scenario simulations. Geosci. Mod. Dev., **13**, 6165-6200. https://doi.org/10.5194/gmd-13-6165-2020.

Sellar, A., C. Jones, J. Mulcahy, Y. Tang, A. Yool, et al., 2019: UKESM1: Description and evaluation of the U.K. Earth System Model. J. Adv. Mod. Earth Sys., **11**, 4513-4558. https://doi.org/10.1029/2019MS001739.

Senatore, A., L. Furnari, G. Nikravesh, J. Castagna, and G. Mendicino, 2026: Increasing daily precipitation extremes despite declining annual totals in southern Europe: a modeling study on the effects of Mediterranean Sea warming. Hydrol. Earth Sys. Sci., **30**, 2913-2930. https://doi.org/10.5194/hess-30-2913-2026.

Streffing, J., T. Semmler, L. Zampieri, and T. Jung, 2021: Response of Northern Hemisphere weather and climate to Arctic sea ice decline: resolution independence in Polar Amplification Model Intercomparison Project (PAMIP) simulations. J. Climate, **34**, 8445-8457. https://doi.org/10.1175/JCLI-D-19-1005.1.

Swapna, P., R. Krishnan, N. Sandeep, A. Prajeesh, D. Ayantika, S. Manmeet, and R. Vellore, 2018: Long-term climate simulations using the IITM Earth System Model (IITM-ESMv2) with focus on the South Asian Monsoon. J. Adv. Mod. Earth Sys., **10**, 1127-1149. https://doi.org/10.1029/2017MS001262.

Swart, N., J. Cole, V. Kharin, M. Lazare, J. Scinocca, et al., 2019: The Canadian Earth System Model version 5 (CanESM5.0.3). Geosci. Mod. Dev., **12**, 4823-4873. https://doi.org/10.5194/gmd-12-4823-2019.

Thompson, V., D. Coumou, V. Galfi, T. Happé, S. Kew, I. Pinto, S. Philip, and H. deVries, 2024: Changing dynamics of Western European summertime cut-off lows: A case study of the July 2021 flood event. Atmos. Sci. Lett., **25**(10), e1260. https://doi.org/10.1002/asl.21260.

Tuel, A., and E. Eltahir, 2020: Why Is the Mediterranean a climate change hot spot? J. Clim. **33**, 5829–5843. https://doi.org/10.1175/JCLI-D-19-0910.1.

Valenzuela, R., R. Garreaud, I. Vergara, D. Campos, M. Viale, and R. Rondanelli, 2022: An extraordinary dry season precipitation event in the subtropical Andes: drivers, impacts and predictability. Wea. Cli. Extr., **37**, 100472. https://doi.org/10.1016/j.wace.2022.100472.

Vecchi, G., T. Delworth, H. Murakami, S. Underwood, A. Wittenberg, F. Zeng, and coauthors, 2019: Tropical cyclone sensitivities to CO2 doubling: roles of atmospheric resolution, synoptic variability and background climate changes. Cli. Dyn, **53**, 5999-6033. https://doi.org/10.1007/s00382-019-04913-y.

Voldoire, A., D. Saint-Martin, S. Sénési, B. Decharme, A. Alias, et al., 2019: Evaluation of CMIP6 DECK experiments with CNRM-CM6-1. J. Adv. Mod. Earth Sys., **11**, 2177-2213. https://doi.org/10.1029/2019MS001683.

Volodin, E., E. Mortikov, S. Kostrykin, V. Galin, V. Lykossov, et al., 2017: Simulation of the present-day climate with the climate model INMCM5. Cli. Dyn., **49**, 3715-3734. https://doi.org/10.1007/s00382-017-3539-7.

https://doi.org/10.5194/egusphere-2026-4187
Preprint. Discussion started: 7 August 2026

Wu, T., R. Yu, Y. Lu, W. Jie, Y. Fang, et al., 2021: BCC-CSM2-HR: a high-resolution version of the Beijing Climate Center Climate System Model. Geosci. Mod. Dev., **14**, 2977-3006. https://doi.org/10.5194/gmd-14-2977-2021.

Xavier, P., M. Willett, T. Graham, P. Earnshaw, D. Copsey, and coauthors, 2023: Assessment of the Met Office Global Coupled model version 5 (GC5) configurations. Report Met Office, Exeter. pp41. Available at https://centaur.reading.ac.uk/112173/. [Last accessed 17 June 2026].

Yamamoto, K., K. Iga, and A. Yamazaki, 2024: Mergers as the maintenance mechanism of cutoff lows: a case study over Europe in July 2021. Mon. Wea. Rev., **152**, 1241-1256. https://doi.org/10.1175/MWR-D-23-0024.1.

Yuan, P., R. van Malderen, X. Yin, H. Vogelmann, W. Jiang, J. Awange, B. Heck, and H. Kutterer, 2023: Characterisations of Europe's integrated water vapour and assessments of atmospheric reanalyses using more than 2 decades of ground-based GPS. Atmos. Chem. Phys., **23**, 3517-3541. https://doi.org/10.5194/acp-23-3517-2023.

Yukimoto, S., H. Kawai, T. Koshiro, N. Oshima, et al., 2019: The Meteorological Research Institute Earth System Model version 2.0, MRI-ESM2.0: Description and basic evaluation of the physical component. J. Roy. Met. Soc. Japan, **97**, 931-965. https://doi.org/10.2151/jmsj.2019-051.

Zappa, G., M. Hawcroft, L. Shaffrey, E. Black, and D. Brayshaw, 2015: Extratropical cyclones and the projected decline of winter Mediterranean precipitation in the CMIP5 models. Clim. Dyn., **45**, 1727–1738. https://doi.org/10.1007/s00382-014-2426-8.